Biogeosciences Discuss., doi:10.5194/bg-2017-181, 2017
Manuscript under review for journal Biogeosciences
Discussion started: 19 May 2017

Biogeosciences Discussions Open Access EGU

Flocculation of dissolved organic matter controls the distribution of iron in boreal estuarine sediments

Tom Jilbert[1,2], Eero Asmala[3], Christian Schröder[4], Rosa Tiihonen[1], Jukka-Pekka Myllykangas[1], Joonas J. Virtasalo[5], Aarno Kotilainen[5], Pasi Peltola[6], Päivi Ekholm[7], and Susanna Hietanen[1,2]

[1]Department of Environmental Sciences, Faculty of Biological and Environmental Sciences, University of Helsinki, P.O. Box 65, 00014 University of Helsinki, Finland
[2]Tvärminne Zoological Station, University of Helsinki, J.A. Palménintie 260, 10900 Hanko, Finland
[3]Department of Bioscience -Applied Marine Ecology and Modelling, Aarhus University, Frederiksborgvej 399, 4000 Roskilde, Denmark
[4]Biological and Environmental Sciences, Faculty of Natural Sciences, University of Stirling, Stirling FK9 4LA, Scotland, United Kingdom
[5]Marine Geology, Geological Survey of Finland (GTK), P.O. Box 96, 02151 Espoo, Finland
[6] Boliden Rönnskär, 932 81 Skelleftehamn, Sweden
[7]Department of Food and Environmental Sciences, P.O. Box 66, 00014 University of Helsinki, Finland

Correspondence to: Tom Jilbert (tom.jilbert@helsinki.fi)

Biogeosciences Discuss., doi:10.5194/bg-2017-181, 2017
Manuscript under review for journal Biogeosciences
Discussion started: 19 May 2017

Abstract. Iron (Fe) plays a key role in sedimentary diagenetic processes in coastal systems, participating in various redox reactions and influencing the burial of organic carbon. Large amounts of Fe enter the marine environment from boreal river catchments associated with dissolved organic matter (DOM). However, the fate of this Fe pool in estuarine sediments has not been extensively studied. Here we show that flocculation of DOM along salinity gradients in an estuary of the northern Baltic Sea efficiently transfers Fe from the dissolved phase into particulate material that accumulates in the sediments. Consequently, we observe a decline with distance offshore in both the Fe content of the sediments and proportion of terrestrial material in the sedimentary organic matter pool. Mössbauer spectroscopy and sequential extractions suggest that large amounts of Fe in sediments of the upper estuarine zone are associated with organic matter as unsulfidized Fe (II) complexes, or present in the form of ferrihydrite, implying a direct transfer of flocculated material to the sediments. Accordingly, the contribution of these components to the total sedimentary Fe declines with distance offshore while other Fe phases become proportionally more important. Sediment core records show that the observed lateral distribution of Fe minerals has remained similar over recent decades, despite variable Fe inputs from anthropogenic sources and eutrophication of the coastal zone. Pore water data suggest that the vertical zonation of diagenetic processes in the sediments is influenced by both the availability of Fe and by bottom water salinity, which controls the availability of sulfate (SO_4^{2-}).

Biogeosciences Discuss., doi:10.5194/bg-2017-181, 2017
Manuscript under review for journal Biogeosciences
Discussion started: 19 May 2017

1 Introduction

Iron (Fe) is present in marine and freshwater sediments in a wide range of phases. Reactive Fe minerals, such as oxides, sulfides, phosphates and carbonates, are involved in diagenetic reactions in sediments and consequently influence the cycling of carbon and nutrients (e.g., Berner, 1970; Slomp et al., 1996a,b; Lovley et al., 2004; Jilbert and Slomp, 2013; Kraal et al., 2015; Robertson et al., 2016). Iron has also recently been shown to stabilize organic carbon in sediments, promoting carbon burial (Lalonde et al., 2012; Shields et al., 2016). Hence, the lateral and vertical distribution of Fe in sediments is important for broader biogeochemical cycles. Critical to understanding the distribution of sedimentary Fe is a knowledge of the processes converting Fe between its various forms, and how they vary spatially in aquatic systems.

In boreal terrestrial environments, Fe is released during the chemical weathering of Fe-bearing minerals in soils. These include silicates in the fine fraction of till (Lahermo et al., 1996), and, especially in areas overlain with late- or post-glacial lacustrine and brackish water sediments, reactive Fe minerals (Virtasalo and Kotilainen, 2008). During weathering under oxic conditions in the absence of organic ligands, Fe (II) is quickly oxidized to Fe (III), which in turn precipitates as oxides (Schwertmann and Taylor, 1977). Typically, the first-formed oxide mineral is amorphous, highly reactive ferrihydrite ($Fe^{3+}_{4–5}(OH,O)_{12}$), which may subsequently mature into crystalline oxides such as goethite and hematite (Raiswell, 2011). Although such maturation is rapid in tropical and temperate systems, under the cold, low pH conditions of boreal aquatic environments its half-life may be several years (Schwertmann et al., 2004).

Weathering of Fe in boreal systems also frequently occurs under anoxic conditions, in the presence of dissolved organic compounds such as humic and fulvic acids (Krachler et al., 2016), for example in peatland environments. These compounds are effective chelators of dissolved Fe, and form complexes with Fe (II) in anoxic soil solution (Sundman et al., 2014). Such complexes are typically nanoparticulate–colloidal in size and hence pass through 0.2–0.45 µm pore-size filters, to operationally classify as dissolved material. The stability of Fe (II)-organic complexes in river systems depends on the concentration of chelating organic compounds and the time available for oxidation (Ingri and Conrad, 2015). Typically, dissolved Fe in upstream areas of boreal catchments is dominated by Fe (III)-organic complexes, while increasing pH conditions further downstream may convert the Fe in these complexes to ferrihydrite (Neubauer et al., 2013). Ferrihydrite itself is nanoparticulate (Raiswell, 2011), and its high surface area and density of hydroxyl groups favor continued association with DOM colloids via sorption (Dzombak et al., 1990; Eusterhues et al., 2008).

In estuarine environments, elevated electrolyte strength along salinity gradients induces the flocculation of DOM (Sholkovitz et al. 1978) and associated Fe (Boyle et al., 1977) from river waters. This phenomenon is usually explained by the cation-induced coagulation of colloidal humic substances, which carry a negative surface charge (Eckert and Sholkovitz 1976). Flocculation is typically selective for humic substances of high molecular weight and larger colloidal particle size (Uher et al., 2001; Asmala et al., 2014). Consequently, the ‘truly dissolved’ Fe which passes through the flocculation zone of estuaries

(e.g., Dai and Martin, 1995) is associated with DOM of lower molecular weight and smaller colloidal particle size (e.g., < 3 nm), most likely in the form of fulvic acids (Stolpe and Hassellöv, 2007). This component may be more substantial than previously thought and hence play a role in providing Fe as a micronutrient to the oceans (Kritzberg et al., 2014; Krachler et al., 2016). However, the majority of dissolved Fe in river water is associated with higher-molecular weight DOM, hence most riverine dissolved Fe is retained by flocculation in estuaries (Raiswell, 2011).

Together with the deposition of riverine particulate Fe close to river mouths (Poulton and Raiswell, 2002, Li et al., 2016), flocculation may be expected to act as an important mechanism of Fe sedimentation in the coastal zone. The role of flocculation in Fe sedimentation may be enhanced in boreal estuarine systems, where high DOM fluxes maintain a relatively large component of riverine Fe in the dissolved phase (Kritzberg et al., 2014). However, few studies have attempted to investigate the connection between flocculation and the Fe distribution in boreal estuarine sediments. This is a significant gap in existing knowledge, since an increasing number of studies have demonstrated the importance of reactive Fe minerals in sedimentary diagenesis in boreal coastal areas, including their roles in the anaerobic oxidation of methane (AOM) (Slomp et al., 2013; Egger et al., 2015a) and in phosphorus retention in sediments (Reed et al., 2011; Norkko et al., 2012; Egger et al., 2015b). Furthermore, Fe has recently been suggested to play an important role in carbon burial (Lalonde et al., 2012; Shields et al., 2016) and nitrogen cycling (Robertson et al., 2016) in marine sediments.

Understanding the distribution of Fe minerals in boreal sedimentary environments will improve our knowledge of the broader role of Fe in sediment biogeochemistry. Here we present a combined study of water column, sediment and pore water chemistry in a non-tidal estuarine system in the northern Baltic Sea, to investigate the impact of DOM flocculation on the distribution of Fe in boreal coastal sediments. In the estuarine water column, we study the distribution of dissolved and particulate Fe and organic matter, to assess the transfer of these components from the dissolved to particulate phase along the salinity gradient. Using sediment core data from selected locations, we show how processes in the water column control the lateral distribution of Fe and organic matter in estuarine sediments. Furthermore, we investigate the degree to which these processes have remained stable during recent changes in nutrient inputs to the coastal zone of the Baltic, and industrial activity in the vicinity of our study sites. Finally, we demonstrate how the lateral distribution of Fe, together with salinity and redox gradients, influences the vertical diagenetic zonation of the sediments along the estuarine transect.

2 Study location

The Finnish coastline of the western Gulf of Finland and Archipelago Sea (northern Baltic Sea) is characterized by a mosaic of islands and small bays, intersected by a network of channel-like, non-tidal estuaries (Fig. 1a). The undulating mosaic represents the bedrock surface known as the pre-Cambrian peneplain (Winterhalter et al., 1981), while the channels correspond to fault lines in the bedrock (Hausen, 1948; Virtasalo et al., 2005). The entire area was covered by the Fennoscandian continental ice-sheet during the last glacial (Weichselian) maximum. The ice-margin retreat from the area ca. 12 ka ago was

Biogeosciences Discuss., doi:10.5194/bg-2017-181, 2017
Manuscript under review for journal Biogeosciences
Discussion started: 19 May 2017

followed by the successive deposition of till, outwash, glaciolacustrine rhythmite, patchily-distributed debrites, postglacial lacustrine clay and brackish-water mud drift (Virtasalo et al., 2007). These deposits provide the source material for mobile Fe in the drainage basins of southern Finland, and each deposit has a distinct Fe mineralogy (Virtasalo and Kotilainen, 2008).

The principal study area is the estuary of the Mustionjoki river and its adjacent archipelago (Fig. 1a). This river and its estuary appear under several alternative Finnish-, Swedish- and English- language names in cartographic material and the scientific literature, including Karjaanjoki (e.g., Asmala et al., 2014), Pohjanpitäjänlahti (e.g., Virta, 1977), Pojoviken (e.g., Niemi, 1977) and Pojo Bay. The First Salpausselkä ice-marginal formation intersects the estuary close to the town of Ekenäs (Fig. 1a). The First Salpausselkä forms a shallow sill of < 10m water depth, separating the inner basin of the estuary (maximum water depth 39 m) from the slope of the archipelago towards the open Gulf of Finland (Fig. 1b).

3 Materials and methods

3.1 Hydrographic profiling

Over 2 days of sampling onboard R/V Saduria and R/V J.A. Palmén in June 2015, water column temperature, salinity and dissolved oxygen profiles were collected at stations A–K in the estuary of the Mustionjoki river and adjacent archipelago, using multiparameter water quality sondes (YSI™ CTD with optical oxygen sensor and Valeport MiniCTD). The 11 vertical profiles for each parameter were interpolated into cross-sectional contour plots using the Sigmaplot™ software package (Fig. 1b). Station A is situated at the mouth of the Mustionjoki river, while station K is situated 33 km due S of the river mouth (~40 km absolute distance along transect) in the open Gulf of Finland. The precise locations of the stations were selected on the basis of suitability for sediment sampling; all are situated in 10–100 m-scale bathymetric depressions where soft sediments are expected to accumulate.

3.2 Sampling and analysis of suspended particulate organic matter

During the sampling campaign in June 2015, discrete water samples were collected at 5 m depth intervals at stations A–K in the estuary of the Mustionjoki river and adjacent archipelago, using a 5 L Limnos™ water sampler. Water samples were transferred onboard to acid-washed polyethylene bottles, stored at 4°C and filtered within 48 hours of sampling at Tvärminne Zoological Station, Hanko, Finland. One 500 ml aliquot of each sample was filtered through pre-weighed, pre-combusted (450°C for 4 h) Whatman® GF/F filters (nominal pore size 0.7 µm). GF/F filters were freeze-dried and re-weighed to estimate total suspended solids (TSS). Total carbon (C_{tot}) and total nitrogen (N_{tot}) on the filters, and the stable isotopic ratio of carbon relative to the Vienna Pee Dee Belemnite ($\delta^{13}C$), were estimated by thermal combustion elemental analysis-mass spectrometry (TCEA-MS) at Tvärminne Zoological Station. Precision and accuracy of all parameters as checked by in-house and reference standards was < 2.5% relative standard deviation (RSD). Particulate inorganic carbon and nitrogen are assumed insignificant in this setting, hence C_{tot}. and N_{tot}. are assumed equal to organic carbon and nitrogen, respectively (C_{org} and N_{org}).

Biogeosciences Discuss., doi:10.5194/bg-2017-181, 2017
Manuscript under review for journal Biogeosciences
Discussion started: 19 May 2017

3.3 Sampling and analysis of particulate and dissolved Fe

During the sampling campaign in June 2015, two additional 250 ml aliquots of water from each sample were filtered through parallel Whatman^{R} Nuclepore track-etched polycarbonate membrane filters (pore size 0.4 µm). Filtrate was collected in 15 ml centrifuge tubes and acidified to 1M HNO_3 for analysis of dissolved Fe and other elements by ICP-MS at University of Helsinki Department of Geosciences and Geography. Filters were freeze-dried and acid-digested in Teflon^{TM} vessels (digestion in 2.5 mL HF + 2.5 mL $HClO_4/HNO_3$ at volumetric ratio 3:2, reflux at 90°C for 12 h, followed by evaporation of acids until gel texture and re-dissolution in 20 mL 1M Suprapur^{R} HNO_3). Analysis of particulate Fe (among other elements) in the resulting digests was performed by ICP-OES at University of Helsinki Department of Food and Environmental Sciences (precision and accuracy < 5% RSD as determined by in-house and reference standards). Values were converted to µmol L^{-1} using TSS estimates from the corresponding GF/F filter.

3.4 Sediment sampling

In September 2014 onboard R/V Saduria, sediments were collected from stations A–K on the Mustionjoki estuary transect using a GEMAX^{TM} short gravity corer (internal diameter 9 cm, core length 30–60 cm). Four to five sediment slices of 2 cm thickness, evenly spaced with depth over the full length of the core, were obtained from each station (e.g., station K: 0–2 cm; 8.5–10.5 cm, 17–19 cm, 25.5–27.5 cm, 34–36 cm). During sampling campaigns in 2015, GEMAX^{TM} cores were taken from stations A, D (June) and J (April, June) and sliced completely at 1 cm resolution (0–10 cm depth) and 2 cm resolution (10 cm depth–core base). In all campaigns, whole sediment slices were transferred immediately to plastic bags, dipped in water to seal the bag, and deposited in a gas-tight jar that was flushed with nitrogen within 1 h of sampling and stored dark at 4°C. Due to the large volume of tightly-packed sediment in each jar, visible oxidation effects during sampling were minimal. Subsamples of wet sediment slices were obtained under nitrogen atmosphere, frozen, freeze-dried and homogenized, and stored in N_2-filled gas-tight jars until further processing.

3.5 Analysis of sedimentary organic matter

Selected sediment samples were prepared for analysis of sedimentary organic matter. Sub-samples of dried, powdered sediments were weighed into aluminium capsules. Total sedimentary carbon (C_{tot}) and nitrogen (N_{tot}), and the stable isotopic ratio of carbon reported relative to Vienna Pee Dee Belemnite ($\delta^{13}C$), were estimated by thermal combustion elemental analysis-mass spectrometry (TCEA-MS) at Tvärminne Zoological Station and University of California, Davis, USA. Precision and accuracy of all parameters as checked by in-house and reference standards was < 2.5% RSD. Sedimentary inorganic carbon and nitrogen are assumed insignificant in this setting, hence C_{tot} and N_{tot} are assumed equal to organic carbon and nitrogen, respectively (C_{org} and N_{org}).

Biogeosciences Discuss., doi:10.5194/bg-2017-181, 2017
Manuscript under review for journal Biogeosciences
Discussion started: 19 May 2017

3.6 Quantification of organic matter sources

A simple two-component mixing model was applied for a first-order quantification of the relative contributions of terrestrial plant-derived organic material ($\%OC_{terr}$), vs. riverine–estuarine phytoplankton ($\%OC_{phyt}$), to total organic matter in both water column and sediment samples. The calculation uses only the molar N/C ratio of organic matter, and end-member values, N/C_{EM}, based on the study of Goñi et al. (2003):

$$\%OC_{phyt} = \frac{\left(N/C_{sample} - N/C_{EM-terr}\right)}{\left(N/C_{EM-phyt} - N/C_{EM-terr}\right)} \times 100 \quad (1)$$

$$\%OC_{terr} = 100 - \%OC_{phyt} \quad (2)$$

where $N/C_{EM\text{-}terr} = 0.04$, and $N/C_{EM\text{-}phyt} = 0.13$. The calculation assumes that plant matter and phytoplankton are the only sources of organic material present in the samples, that their N/C values are spatially and temporally fixed at the end-member values, and that these values do not alter significantly during sedimentation and burial of organic matter. Fields in N/C vs. $\delta^{13}C$ space, also taken from Goñi et al. (2003) and corresponding to riverine–estuarine phytoplankton, marine phytoplankton, and terrestrial C3 plants respectively, were used in the interpretation of the data.

3.7 Analysis of sedimentary Fe, S and Pb by ICP-OES

Selected sediment samples were prepared for ICP-OES analysis. Sub-samples of dried, powdered sediments were weighed into Teflon digestion vessels and digested in an acid cocktail (digestion in 2.5mL HF + 2.5 mL $HClO_4/HNO_3$ at volumetric ratio 3:2, reflux at 90°C for 12 h, followed by evaporation of acids until gel texture and re-dissolution in 20 mL 1M Suprapur^R HNO_3). ICP-OES analysis for total Fe, sulfur (S) and lead (Pb), among other elements, was performed at University of Helsinki Department of Food and Environmental Sciences (precision and accuracy < 5% as determined by in-house and reference standards).

3.8 Estimate of sedimentation rates using sedimentary Pb profiles

Sedimentation rates for stations A, D and J were estimated on the basis of total Pb (Pb_{tot}) profiles measured on the three GEMAX^{TM} cores from 2015. Each core profile showed a distinct peak in Pb_{tot} (Supplementary Figure 1) which was assigned to the year 1970 (Renberg et al., 2001; Zillen et al., 2012). A first order estimate of sedimentation rate was calculated assuming constant mass accumulation over the period 1970–2015.

Biogeosciences Discuss., doi:10.5194/bg-2017-181, 2017
Manuscript under review for journal Biogeosciences
Discussion started: 19 May 2017

3.9 Sequential extraction and analysis of sedimentary Fe phases

Selected sediment samples were subjected to the sequential extraction procedure for Fe described by Poulton and Canfield (2005). Sub-samples of dried, powdered sediments were weighed into extraction vessels and a series of reagents was applied (Table 2). After each addition, samples were placed in an orbital shaker for the duration of the extraction, then centrifuged at 3000 rpm for 5 minutes before decanting the supernatant. To limit the risk of oxidation affecting the Fe speciation during the extraction, stages 1–4 of the extraction procedure were performed under nitrogen atmosphere, and reagents were purged with nitrogen for 30 mins prior to addition to the samples. All supernatants were analyzed for Fe (among other elements) by Microwave Plasma-Atomic Emission Spectroscopy (MP-AES) at University of Helsinki Department of Geosciences and Geography. Replicate extraction of parallel samples yielded RSD values of < 15% for all stages of the procedure.

The Poulton and Canfield (2005) protocol does not include an explicit stage for the extraction of Fe from sulfide minerals. For the purposes of this study, we assumed the dominant sulfide mineral present in the samples to be pyrite (FeS_2), which is insoluble in stages 1–5 of the protocol (Poulton and Canfield, 2005). Hence, we estimated the contribution of sulfide-bound Fe to total Fe according to:

$$Sulfide\ Fe = 0.5 \times Total\ S \text{ (all units µmol g}^{-1}\text{)} \quad (3)$$

This is a conscious approximation, since sediments from this region are known to also contain iron monosulfide (FeS) (e.g., Egger et al., 2015a, Yu et al., 2015); however the approximation has no bearing on the main conclusions of the study. The sum of the 5 stages of the sequential extraction procedure, plus the estimated contribution of sulfide-bound Fe, were subtracted form total Fe as determined by ICP-OES, to estimate residual (non-soluble) Fe, assumed to be present in unreactive silicate minerals:

$$Residual\ Fe = Total\ Fe - \sum Stages\ 1\ to\ 5 - Sulfide\ Fe \text{ (all units µmol g}^{-1}\text{)} \quad (4)$$

3.10 Mössbauer spectroscopy of sedimentary Fe phases

Surface sediment samples (0–1 cm) from stations A and D sampled in June 2015 were prepared for Mössbauer spectroscopy. Sub-samples of dried, powdered sediments (station A: 52 ±9 mg; station D: 97 ±9 mg) were placed in acrylic glass tubs with a circular cross section of ~1 cm². Mössbauer spectra were collected using a miniaturized Mössbauer spectrometer MIMOS II (Klingelhöfer et al. 2003) with a ^{57}Co in Rh matrix radiation source in constant acceleration mode. The source had an activity of ~1.4 GBq and the instrument was set up in backscattering geometry. Measurements were performed at room temperature. Spectra were calibrated against alpha-iron at room temperature and fitted with an in-house routine (Mbfit) using Lorentzian line profiles. Mbfit is based on the least-squares minimization routine MINUIT (James 2004). Quantification of iron-bearing phases and iron oxidation states is based on relative subspectral areas. No f-factor correction was applied.

Biogeosciences Discuss., doi:10.5194/bg-2017-181, 2017
Manuscript under review for journal Biogeosciences
Discussion started: 19 May 2017

3.11 Pore water sampling

Prior to sediment slicing during the June 2015 campaign, pore water was sampled through pre-drilled holes (⌀ 4 mm) in the GEMAX™ coring tubes, using Rhizons™ mounted on a purpose-built plastic rack. Two parallel series of samples (vertical resolution 2 cm) were obtained for each core; one for analysis by ICP-OES, the other for analysis of dissolved hydrogen sulfide (H_2S). Samples were collected in polyethylene syringes connected directly to the Rhizons™, which were held open by a wooden spacer to create a vacuum. The syringes of the H_2S series were pre-filled with 1 ml 10% zinc acetate solution to trap sulfide as ZnS. All samples were transferred from the syringes to 15 ml centrifuge tubes in the laboratory within 2 h of sampling. From the first series, a sub-sample for ICP-OES analysis was taken immediately and acidified to 1 M HNO_3. A parallel GEMAX™ core, pre-drilled with holes of ⌀ 15 mm, was used for sampling for dissolved methane (CH_4). 10 ml wet sediment was collected through each hole using a cut-off syringe and transferred to a 65 ml glass vial filled with saturated NaCl solution (Egger et al., 2015a). Vials were capped with a rubber stopper, and a headspace of 10 ml N_2 (quality 5.0) was injected using a gas-tight glass syringe. Methane in pore waters was assumed to be quantitatively salted out into the headspace during equilibration (O'Sullivan and Smith, 1970). Samples were stored upside-down until analysis such that headspace gas was not in contact with the rubber stopper.

3.12 Pore water analysis

Acidified pore water sub-samples from the first series of Rhizons™ were analyzed for total Fe and S, among other elements, by ICP-OES at University of Helsinki Department of Food and Environmental Sciences. Iron is assumed to be present in pore waters as Fe^{2+}, while S is assumed to represent SO_4^{2-} only, due to the loss of H_2S during sample acidification (Jilbert and Slomp, 2013). H_2S concentrations in pore water samples from the second series of Rhizons™ were determined by spectrophotometry (670 nm) after direct addition of an acidic solution of $FeCl_3$ and n,n-dimethyl-p-phenylenediamine (Cline, 1969; Reese et al., 2011) to the sample vials. This procedure dissolves the ZnS precipitate and immediately complexes S as methylene blue for spectrophotometric analysis. H_2S concentrations were calibrated against a series of standard solutions of $Na_2S.3H_2O$, fixed in Zn acetate in the same manner as the samples. The exact concentration of S in the $Na_2S.3H_2O$ stock solution was determined by iodometric titration (Burton et al., 2008).

For analysis of dissolved CH_4, 1 ml headspace gas was sampled from the 65 ml vials using a gas-tight glass syringe. An equivalent volume of salt solution was allowed to flow into the vial through a parallel syringe to equalize pressure in the headspace. Gas samples were then injected into 12 mL gas-tight glass Exetainer™ vials (LabCo model 839W). An additional 20 mL N_2 gas was injected into the Exetainers to generate overpressure prior to analysis. CH_4 concentrations were analyzed using an Agilent Technologies 7890B gas chromatograph (GC) at University of Helsinki Department of Environmental Sciences, equipped with flame ionization detector (FID) at 250°C, oven temperature 60°C, 2.4 m Hayesep Q column with 1/8" connection, 80/100 mesh range, 1.0 mL sample loop and helium carrier gas at flow rate 21 mL min^{-1}. Raw peak area data were

converted to mole fraction (ppm) using a 4-point linear calibration of standard gas mixtures (certified concentrations ± 2%) and blanks, analyzed prior to each sample series. Single standards were analyzed after every 10 samples to monitor within-series drift, which was observed to be negligible. Concentrations in the pore water of the original 10 ml wet sediment sample were back-calculated assuming a constant porosity of 90%.

3.13 Additional supporting data

N/C and $\delta^{13}C$ of DOM was measured from surface-water samples from six locations along the Mustionjoki estuary transect (stations *a–f*, Fig. 1a) during three sampling campaigns (April, August and October) in the year 2011, as reported in Asmala et al. (2014) and Asmala et al. (2016). Sampling locations are given in Table 1.

Surface sediment (0–1 cm) total Fe and Al data was generated for six locations in the estuary of the Paimionjoki river and its adjacent archipelago (stations L–Q, Fig. 1a). Samples were obtained in August and September 2001 during a 94-station survey of Archipelago Sea sediments, as reported in the studies of Virtasalo et al. (2005) and Peltola et al. (2011). For comparability with the present study, new subsamples of this material were digested and analyzed as outlined above. The locations and water depths of stations L–Q are given in Table 1.

4 Results

4.1 Hydrography of the transect

At the time of the primary sampling campaign in June 2015, the water column in the estuary of the Mustinojoki river and the adjacent archipelago was strongly stratified. Strong vertical temperature stratification was evident throughout the transect (Fig. 1b, top), while strong salinity stratification was also present in the inner basin of the estuary (Fig. 1b, middle). The freshwater input from the Mustionjoki river was sufficient to generate a surface-water lens of salinity 0–2 extending across the entire inner basin north of the First Salpausselkä, which forms the sill at Ekenäs. The halocline shallowed towards the sill, and the salinity isolines between stations C and G were strongly inclined. Deep waters upstream of the sill showed depleted concentrations of dissolved oxygen relative to surface-water values (7–8 mg L^{-1} vs. 10–11 mg L^{-1}).

4.2 Dissolved and particulate Fe in the water column

Dissolved Fe concentrations in the surface water at the mouth of the Mustionjoki river in June 2015 (station A, salinity 1.0) were 1.3 µmol L^{-1} (Fig. 2a). Concentrations decreased offshore to values around 0.02 µmol/L in the open waters of the Gulf of Finland (station K). The isolines of [Fe_{diss}] in the estuarine water column were inclined similarly to those of salinity (Fig. 1b), with a relatively deep surface layer of Fe-rich waters at the river mouth shallowing towards the sill at Ekenäs. However,

Biogeosciences Discuss., doi:10.5194/bg-2017-181, 2017
Manuscript under review for journal Biogeosciences
Discussion started: 19 May 2017

surface water salinity and [Fe_{diss}] along the transect show a strongly non-linear relationship, suggesting non-conservative mixing between river and offshore water with respect to [Fe_{diss}], due to removal of Fe_{diss} from solution (Fig. 2b).

Particulate Fe in the water column of the estuary in June 2015 showed a contrasting distribution to that of [Fe_{diss}] (Fig. 2a). Although maximum [Fe_{part}] was also observed at the river mouth (3.9 µmol L^{-1} in surface waters at station A), values decreased rapidly within a short distance offshore (station B surface water = 1.4 µmol L^{-1}; station B, 5 m depth = 0.6 µmol L^{-1}). Further away from the river mouth, [Fe_{part}] showed higher values in a zone extending from 15 m depth at station C to the surface waters at station G (Fig. 2a), approximately coinciding with the halocline of salinity = 2–4 (Fig. 1b). In the archipelago region of the transect (stations G–J), [Fe_{part}] declined gradually offshore.

4.3 Particulate organic matter in the water column

Particulate organic carbon (POC) and nitrogen (PON) concentrations in the water column of the estuary in June 2015 ranged from 5–75 µmol L^{-1} and 0.5–7 µmol L^{-1}, respectively, and were consistently highest in surface waters (not shown). Moreover, surface waters throughout the transect were characterized by a relative enrichment of N (N/C = 0.14–0.17, Fig. 3a). In contrast, deeper waters had lower concentrations of particulate organic matter and a relative depletion of N (N/C = 0.08–0.13). The region close to the river mouth displayed the most pronounced N/C enrichments anywhere on the transect.

The distribution of $\delta^{13}C_{POC}$ showed a general similarity to that of N/C. Relatively depleted values were observed in surface waters (-29‰ – -31‰), with the most depleted values observed close to the river mouth, while deep water values were relatively enriched (-26‰ – -28‰) (Fig. 3a, bottom). One anomalous sample of relatively enriched values (approx. -26‰) was observed in the surface waters at site G, close to the sill at Ekenäs. When N/C and $\delta^{13}C_{POC}$ values are plotted in x-y space, surface water samples for most stations, regardless of salinity, plot close to the riverine end of the riverine–estuarine phytoplankton continuum. At each site, samples from deeper in the water column trend away from this region of the diagram towards the field corresponding to terrestrial C3 plants (Fig. 3b).

4.4 Sedimentary organic matter along the transect

Mean total organic carbon (C_{org}) contents of the upper 30–50 cm of sediments sampled in September 2014 were close to 4% dry weight at stations A–D in the inner Mustionjoki estuary (Fig. 4b). Stations E–G in the vicinity of the sill at Ekenäs showed lower values (e.g. station F = 2.2%), while stations in the archipelago and offshore region (H–G) showed the highest values anywhere on the transect (4%–5%). The four samples from site A, at the mouth of the Mustionjoki river, all showed molar N/C ratios of 0.05–0.09 and $\delta^{13}C_{org}$ of -26‰ – -29‰, hence plot close to the terrestrial C3 plants field in N/C vs. $\delta^{13}C_{org}$ space (Fig. 4a). With increasing distance along the transect, mean N/C and $\delta^{13}C_{org}$ values of sediments from successive stations trend towards the riverine–estuarine phytoplankton continuum. Samples from station K showed molar N/C ratios of 0.12–0.14 and $\delta^{13}C_{org}$ of -23‰ – -24‰, close to the estuarine end of the continuum. Variation of values between different depth intervals

Biogeosciences Discuss., doi:10.5194/bg-2017-181, 2017
Manuscript under review for journal Biogeosciences
Discussion started: 19 May 2017

within each sediment core was substantially less (N/C < 0.04, $\delta^{13}C_{org}$ < 2‰) than between the mean values of station A and station K.

The computed contributions of terrestrial plant-derived and phytoplankton-derived organic matter to sedimentary C_{org} vary systematically along the transect. Based on the assumed end-member values, >70% of sedimentary C_{org} at station A is derived from terrestrial plant material, whereas sedimentary C_{org} at station K is entirely phytoplankton-derived. The rate of change in $\%OC_{terr.}$ and $\%OC_{phyt.}$ between successive stations is greatest from stations A–C, close to the mouth of the Mustionjoki river.

4.5 Sedimentary Fe along the transect

Surface-sediment Fe concentrations were highest at stations A–D in the inner estuary, with a maximum recorded value of >1600 µmol g^{-1} at station B (Fig. 4b). A general trend of decreasing Fe concentrations offshore from station B was observed, to values of approx. 800 µmol g^{-1} at station K. Anomalously low values were observed at station F, coincident with the observed minimum in C_{org} content at this location. The Fe speciation of the surface sediments at stations A and B was dominated by Stages 3 and 4 of the sequential extraction protocol, while Stages 1 and 2 of the protocol were most dominant at station D (Fig. 4b).

^{57}Fe Mössbauer spectroscopy data from surface sediment samples from stations A and D (0–1 cm, June 2015) show markedly contrasting results (Fig. 5; Table 3). The station A spectrum contains an important contribution of an Fe (II) phase which could not be identified from our existing library of minerogenic Fe (II) spectra. The presence of this phase in the sample modulates the relative heights of the major peaks in the spectrum, and generates a distinct shoulder at 1–2 mms^{-1} (Fig. 5). We interpret this phase to represent complexes of non-sulfidized Fe (II) with organic matter (henceforth organic-Fe (II) complexes), which were recently shown to be a major component of sedimentary Fe in a nearby boreal estuary (Yu et al., 2015). The station A spectrum also contains superparamagnetic Fe (III) (interpreted as nanoparticulate ferrihydrite), silicate-bound Fe (II) and a small contribution of magnetite. In contrast, the sample from station D was dominated by superparamagnetic Fe (III) and silicate-bound Fe (II). No Fe carbonate phases (e.g. siderite, ankerite), and no further crystalline oxides (e.g., goethite, hematite or akaganéite) were detected in either sample.

The sequential Fe extraction results for the corresponding samples showed station A to be dominated by Fe soluble in Stages 3 and 4 of the protocol (sodium dithionite and ammonium oxalate-soluble Fe, respectively), which together accounted for >50% of all Fe in the sample (Fig. 5). In contrast, Stages 3 and 4 yielded approximately 20% of all Fe in the samples from station D. Conversely, the contribution of Stages 1 and 2 (sodium acetate-soluble Fe and hydroxylamine-HCl soluble Fe, respectively) to total Fe at station D was greater than for station A.

Biogeosciences Discuss., doi:10.5194/bg-2017-181, 2017
Manuscript under review for journal Biogeosciences
Discussion started: 19 May 2017

4.6 Vertical profiles of sedimentary Fe, C_{org} and S

The along-transect changes in Fe content and speciation persist in the vertical profiles of stations A, D and J (Fig. 6). Background total Fe contents decrease in the order A–D–J (1.0%, 0.8%, 0.5%, respectively), while station A shows a persistently high contribution of dithionite- and oxalate-soluble Fe relative to the other stations. Furthermore the 10–40 cm depth layer in the sediments at station A displays a large enrichment of Fe, peaking at 3% close to the 1970 depth horizon.

The C_{org} profile of station A also differs markedly from those of stations D and J. The station A profile shows generally constant values of ~3% with a small enrichment in the surface sediments, while the station D and J profiles show systematically decreasing C_{org} contents from the surface sediments towards the base of the core. Meanwhile, the S profiles of all three stations show a distinct broad peak in the post-1970 sediments (Fig. 6).

4.7 Vertical profiles of pore water CH_4, SO_4^{2-}, H_2S and Fe^{2+}

At sites A, D and J, a broadly similar vertical zonation can be observed in the pore water chemical profiles, indicating a similar set of diagenetic processes at each site (Fig. 7). CH_4 produced by methanogenesis in the deeper sediments diffuses upwards and reacts with SO_4^{2-} diffusing downwards from the bottom water at the so-called sulfate-methane transition zone (SMTZ) (e.g., Egger et al., 2015a). The reaction

$$CH_{4(aq)} + SO_{4\,(aq)}^{2-} \rightarrow HS_{(aq)}^{-} + HCO_{3\,(aq)}^{-} + H_2O_{(l)} \quad (5)$$

produces H_2S, which accumulates in a distinct peak in the SMTZ. Pore water Fe^{2+}, produced by the reduction of Fe (oxyhydr)oxides in various diagenetic reactions, accumulates above and below the SMTZ. Within the SMTZ itself, the reaction between Fe^{2+} and H_2S

$$Fe_{(aq)}^{2+} + H_2S_{(aq)} \rightarrow FeS_{(s)} + 2H_{(aq)}^{+} \quad (6)$$

efficiently removes Fe^{2+} from the pore waters, and FeS is subsequently converted to pyrite (FeS_2).

However, the profiles from each station differ in terms of the depth, thickness and intensity of the SMTZ. At station A, where bottom water [SO_4^{2-}] is only 1.3 mM, the SMTZ is relatively shallow and narrow. No detectable accumulation of H_2S is observed, while pore water Fe^{2+} shows only a narrow minimum centered on 7 cm depth. At stations D and J, H_2S accumulations in excess of 150 µm L^{-1} are observed in the SMTZ, while Fe concentrations are close to zero between 5 cm and 20 cm depth. Station J, where bottom water [SO_4^{2-}] is 4.8 mM, shows the deepest SMTZ of the three stations as defined by the H_2S peak (centered on 12 cm).

Biogeosciences Discuss., doi:10.5194/bg-2017-181, 2017
Manuscript under review for journal Biogeosciences
Discussion started: 19 May 2017

5 Discussion

5.1 Evidence for DOM flocculation in the estuarine water column and its impact on $Fe_{diss.}$

A recent field and experimental study demonstrated that salinity-mediated flocculation – the aggregation of small particles of organic matter into larger ones under conditions of increasing electrolyte strength – is the dominant process responsible for the loss of DOM along salinity gradients in Finnish estuaries (Asmala et al., 2014). Alternative mechanisms, such as microbial degradation and photolytic mineralization of DOM in the estuarine environment (Dalzell et al., 2009; Moran et al., 2000; Asmala et al., 2013) are considered of lesser importance. Flocculation decreases the fraction of organic matter in the water column which passes through regular filters, and hence decreases the fraction that classifies as DOM. Consequently, negative deviation from conservative mixing is observed when a straight line is drawn between freshwater and offshore end-member values in salinity vs. DOM space (Officer, 1976). However, it should be noted that the conservative mixing approach is sensitive to variations in the end-member values, and quantification of the deviation requires knowledge about the magnitude of this variation (Asmala et al., 2016).

Due to the close association of Fe with DOM in boreal riverine systems, flocculation also strongly influences Fe cycling. The rapid loss of Fe_{diss} observed offshore from the river mouth along the Mustionjoki transect (Fig. 2a) confirms that flocculation removes Fe from solution in this system. The degree of deviation from conservative mixing of Fe_{diss} vs. salinity in Finnish estuaries was shown experimentally to be greater than for DOC (Asmala et al., 2014), suggesting that Fe is preferentially removed relative to bulk DOM. This could indicate a preferred association of Fe with higher molecular weight compounds, which are more sensitive to flocculation (Asmala et al., 2014) or a mechanistic enhancement of flocculation by the presence of Fe (Forsgren et al., 1996).

5.2 The signal of flocculation in suspended POM and $Fe_{part.}$

At the time of sampling in June 2015, POM in surface waters throughout the Mustionjoki estuary and adjacent archipelago was dominated by phytoplankton material, as evidenced by the relatively high N content of POM (circles with letters in Fig. 3a). This strong signal of autochthonous organic material apparently obscures any evidence for POM derived from flocculation of DOM in surface waters at the time of sampling. However, in deeper waters throughout the transect, POM is characterized by lower N contents and more isotopically enriched C. Consequently, deep water POM samples in N/C vs. $\delta^{13}C$ space trend away from the riverine–estuarine phytoplankton continuum and towards the field corresponding to terrestrial C3 plants (Fig. 3b). This suggests that a second fraction of POM contributes to the net N/C and $\delta^{13}C$ values of the deep water samples, and that this fraction has N/C and $\delta^{13}C$ characteristics similar to plant material. We note that this material is unlikely to be resuspended sediment, since its $\delta^{13}C$ values have a much narrower range than those of sedimentary material throughout the transect (Fig. 4a).

Biogeosciences Discuss., doi:10.5194/bg-2017-181, 2017
Manuscript under review for journal Biogeosciences
Discussion started: 19 May 2017

Notably, DOM data from the Mustionjoki estuary cluster close to the terrestrial C3 plants field in N/C vs. $\delta^{13}C$ space (Fig. 3b). The samples in the figure were taken in three separate seasons (April, August, October 2011) and hence approximate the mean composition of DOM in the estuarine system. Assuming negligible fractionation of N/C and $\delta^{13}C$ during flocculation, these results suggest that flocculation of DOM to POM in the estuarine environment may provide the second fraction of POM detected in the N/C_{POM} and $\delta^{13}C_{POM}$ data. The relative abundance of sinking phytoplankton material and flocculation-derived POM then determines the net N/C and $\delta^{13}C$ values measured at any given location in the estuarine water column. Deep water samples display values closer to the flocculation-derived component, likely due to both rapid remineralization of fresh phytoplankton material during settling, and the typically higher salinity of deep waters, which favors the accumulation of flocculated material.

The 2015 Fe_{part} and Fe_{diss} data show clear evidence for the transfer of Fe from the dissolved to the particulate phase as a consequence of flocculation in the Mustionjoki estuary (Fig 2b). When data from all stations and depths are plotted together, $Fe_{part.}$ shows an overall negative deviation from conservative mixing along the salinity gradient. This likely reflects settling of suspended minerogenic matter due to energy dissipation as river water enters the estuarine environment (Syvitski and Murray, 1981), as indicated by a similar trend in suspended particulate aluminum (Al) (not shown). However, samples in the salinity range 2–4 show a clear positive deviation, suggesting an input of Fe_{part} through flocculation of Fe_{diss}. In contrast, Fe_{diss} shows a simple logarithmic non-conservative mixing trend with $R^2 = 0.92$. The concentration of Fe_{part} in the salinity range 2–4 (~1.0 µmol L^{-1}) is similar to that of Fe_{diss} close to the river mouth, suggestive of quantitative transfer of Fe from the dissolved to particulate phase with increasing salinity. The 2D cross-section of Fe_{part} along the transect confirms that a pronounced zone of higher values is observed close to the halocline of the inner estuary, which encompasses the salinity range 2–4 (Fig. 2a). Further offshore, Fe_{part} concentrations decline to a background value of ~0.5 µmol L^{-1}, implying partial settling of the flocculated material to the sediments.

5.3 The impact of flocculation on sedimentary OM and Fe in the upper estuary

The transfer of terrestrially-derived OM and Fe from the dissolved to the particulate phase in the estuarine water column promotes the accumulation of both components in the sediments. Our data show a clear trend of decreasing terrestrial OM and total Fe contents in sediments along the Mustionjoki transect (Fig. 4b). Maximum values are observed at sites A and B, within 2 km due S of the river mouth, implying maximum accumulation of flocculated material in this zone. At first glance this result appears surprising, since the flocculation maximum in the June 2015 data is observed in the halocline of salinity 2–4, located further offshore (Figs. 1, 2). However, the mean annual position of the halocline is likely further upstream (i.e. closer to the river mouth) than recorded during our sampling in June, when discharge in the Gulf of Finland catchment is at its annual maximum (Voipio, 1981). Assuming the suspended particulate maximum and associated gravitational settling to follow the

lateral migration of the halocline through time (Geyer, 1993; Sanford et al., 2001), the focal point of sedimentation for flocculated material may thus be closer to the river mouth than implied by the June 2015 data. Notably, maximum sedimentary Fe concentrations were observed at station B (Fig. 4b), which likely falls close to the intersection of the halocline with the sediment-water interface during mean flow conditions (see Fig. 1). On the other hand, the maximum contribution of terrestrial material to sedimentary OM is recorded at station A. This discrepancy could indicate that settling of riverine suspended microparticulate POM, along with flocculated DOM, contributes to the total sedimentary OM pool at this site. Indeed, organic detritus, including terrestrial plant material, was readily visible in sediment cores from station A.

The speciation of sedimentary Fe at stations A and B contrasts strongly with that at stations further offshore. Stations A and B are characterized by relatively high contributions of dithionite- and oxalate- soluble Fe (Fig. 4b). According to the protocol of Poulton and Canfield (2005), which was originally developed for river sediments, these fractions should represent crystalline Fe oxides such as goethite, akaganéite and hematite (in the dithionite-soluble component) and magnetite (in the oxalate-soluble component). However, of these phases only magnetite is identified in the ^{57}Fe Mössbauer spectrum of the surface sediment from station A (Fig. 5). Moreover, the same spectrum indicates a large contribution of organic-Fe (II) complexes (Fig. 5, Table 3). The behavior of such material in the Poulton and Canfield (2005) protocol has not been previously described, but the large fraction of dithionite- and oxalate- soluble Fe in these samples, coupled to the lack of mineralogical evidence for crystalline oxides, suggest that Stages 3 and 4 of the sequential extraction may be interpreted as primarily indicating organic-Fe (II) complexes in this environment.

The high contents of dithionite- and oxalate- soluble Fe in the sediments of the upper estuary (Fig. 4) thus suggest direct transfer of flocculated Fe-OM aggregates to the sediments, and confirm the suggested role of OM flocculation as a mechanism for trapping Fe in estuaries (Lisistyn, 1995). Flocculated material in the oxic estuarine water column is likely present as Fe (III) partitioned between organic-Fe (III) complexes and ferrihydrite (Neubauer et al., 2013). Reduction of organic-Fe (III) complexes after sedimentation may generate the organic-Fe (II) complexes detected in our sedimentary mineralogical data. Specifically, iron (III) complexed to carboxylate and phenolate functional groups within humic material in the water column may be reduced *in situ* in sediments, retaining its association with these functional groups as demonstrated by X-Ray Absorption Spectroscopy (XAS) (Yu et al., 2015). It is noteworthy that this mechanism for Fe-OM association in sediments differs slightly from that proposed by Lalonde et al. (2012), in which complexes of Fe (III) and relatively labile OM are formed during remineralization of OM in the sediment column and preserved during burial.

Considering the presence of ferrihydrite in flocculated material, flocculation likely also acts as a vector of ferrihydrite to the sediments. Our Mössbauer data detect a large component of superparamagnetic Fe (III), interpreted as nanoparticulate ferrihydrite, in the surface sediments at both stations A and D (Fig. 5, Table 3). Although ferrihydrite is generally thought to be extracted exclusively in Stage 2 of the Poulton and Canfield (2005) protocol (Table 2), the abundance of superparamagnetic Fe (III) in the Mössbauer data, and the absence of carbonate minerals, lead us to conclude that Stages 1 and 2 (Na acetate and

hydroxylamine-HCl) both extract ferrihydrite or similar poorly crystalline Fe (oxyhyr)oxides from the sediments in this setting. Accordingly, the net contribution of Stages 1 and 2 to total extracted Fe in surface sediments generally decreases offshore (Fig. 4a), consistent with a declining input from flocculation.

Notably however, the maximum input of ferrihydrite to sediments occurs at station D, located 7.5 km due S from the river mouth, at the deepest point of the inner estuarine basin. This suggests that focusing of ferrihydrite occurs in the upper estuary, due to redox shuttling effects under seasonally oxygen depleted conditions (e.g., Raiswell and Anderson, 2005; Lenz et al., 2015). Indeed, the Mustionjoki estuary is known to display deep water hypoxia (oxygen concentrations < 2 mg L^{-1}) in the autumn months (Niemi, 1977) and displayed moderate oxygen depletion during our sampling in June 2015 (Fig. 1b). Redox shuttling, and physical reworking of sediments in shallow areas, are known to influence the distribution of both reactive Fe and organic material in the coastal archipelagos of the Baltic Sea, favoring higher concentrations of both components in deeper areas (Virtasalo et al., 2005). Accordingly, the only section of the transect where surface-sediment C_{org} and Fe contents are substantially lower than the whole-transect mean values of 3.5% (C_{org}) and 970 µmol g^{-1} (Fe) are stations F and G, located close to the sill of the First Salpausselkä (Fig. 1b).

5.4 The broader impact of flocculation on sediment biogeochemistry

The enhanced inputs of Fe-OM complexes and ferrihydrite to the sediments in the upper estuary influence diagenetic processes in the sediments, as indicated by the contrasting sediment and pore water chemistry at stations A, D and J (Figs 6, 7). Most importantly, the dominance of terrestrial plant-derived OM at station A lowers the net degradability of OM in the sediments. Humic substances in the flocculated material are derived from complex polymers in vascular plants, such as cellulose, lignin, cutin and cutan (de Leeuw and Largeau, 1993), which are relatively resistant to degradation by the sediment microbial community (e.g. Hedges et al., 2000). The comparatively constant C_{org} content throughout the upper 40 cm at station A (Fig. 6) is consistent with a low range of k-values for net organic matter degradation at this site (see Arndt et al., 2013). In contrast, stations D and J show decreasing C_{org} contents with depth, implying more efficient net degradation of OM (hence a higher range of k-values) due to the proportionally greater input of phytoplankton material at these sites (Fig. 4). Phytoplankton-derived OM contains high concentrations of degradable compounds such as proteins, nucleic acids and simple carbohydrates, and in the shallow estuarine system may be expected to experience relatively little pre-ageing before deposition in the sediments. The abundance of such fresh material thus likely causes the higher net degradability of OM in the sediments at stations D and J (see Arndt et al., 2013). Comparatively low rates of organic matter remineralization in the upper estuary are also reflected in the concentration of primary metabolites in the pore waters. In the sub-SMTZ sediments, maximum concentrations of both methane (Fig. 5) and ammonium (not shown) are significantly lower at station A with respect to the other stations, indicative of lower rates of production of these compounds during organic matter remineralization (e.g., Berg et al., 1998).

Biogeosciences Discuss., doi:10.5194/bg-2017-181, 2017
Manuscript under review for journal Biogeosciences
Discussion started: 19 May 2017

Beyond the impact on sedimentary OM degradability, flocculation also influences the concentration of Fe in the sediment, with potentially important consequences for diagenetic processes. However, the influence of Fe must be considered in the context of changes in bottom water [SO_4^{2-}], due to the close coupling of Fe and S cycling in sediments (Berner, 1970; Berner and Raiswell, 1984). Due to the salinity gradient of the Mustionjoki transect (Fig. 1b), the three sites A–D–J encompass opposing gradients of total sedimentary Fe content and bottom water [SO_4^{2-}] (Figs. 6, 7). At station A, the relative concentration of Fe with respect to SO_4^{2-} is thus at a maximum. Low bottom-water [SO_4^{2-}] leads to a shallow SMTZ (5–10 cm) and despite the production of H_2S during sulfate-mediated AOM (equation 5), no accumulation of H_2S is observed in the pore waters due to the subsequent reaction with Fe^{2+} (equation 6). Conversely, at stations D and J the relative availability of Fe compared to SO_4^{2-} declines, the SMTZ is located progressively deeper, and H_2S accumulates to progressively higher concentrations in the pore waters (Fig. 7). A similar conclusion was predicted for a hypothetical bottom water [SO_4^{2-}] gradient in a recent modeling study focused on the Bothnian Sea (Rooze et al., 2016).

The organic-Fe (II) complexes which dominate sedimentary Fe at station A likely do not participate significantly in the diagenetic reactions determining the pore water chemistry shown in Figure 7. Assuming these complexes to be formed by *in situ* reduction of Fe (III) from Fe (III)-organic complexes after sedimentation (Yu et al., 2015), Fe is retained in the particulate organic phase and not released into the pore waters. Instead, the Fe^{2+} observed in the pore water profiles is likely produced during the reduction of Fe (oxyhydr)oxides, including ferrihydrite, either during dissimilatory reduction coupled to organic matter oxidation (e.g., Canfield et al., 2005):

$$CH_2O_{(s)} + 4Fe(OH)_{3(s)} + 7CO_{2(aq)} \rightarrow 8HCO^-_{3\,(aq)} + 3H_2O_{(l)} + 4Fe^{2+}_{(aq)} \quad (7)$$

or, as recently suggested by various studies (Sivan et al., 2011; Slomp et al., 2013; Egger et al., 2015a), during Fe-mediated anaerobic oxidation of methane (Fe-AOM):

$$CH_{4(aq)} + 8Fe(OH)_{3(s)} + 15H^+_{(aq)} \rightarrow HCO^-_{3\,(aq)} + 21H_2O_{(l)} + 8Fe^{2+}_{(aq)}$$

The higher accumulations of Fe^{2+} in the pore waters of the sub-SMTZ depth interval at stations A and D with respect to station J (Fig. 7) thus indicate higher background rates of Fe (oxyhydr)oxide reduction, consistent with higher net inputs of ferrihydrite to the sediments in the upper estuary (Fig. 4b).

5.5 Temporal stability of flocculation impacts on sedimentation

The coastal zone of the Baltic Sea has been impacted severely by anthropogenic activities during the last century. First of all, enhanced nutrient inputs have altered coastal ecosystems and triggered hypoxia in many areas (Conley et al., 2011). Also land

use changes such as ditching and forest clearance have influenced the inputs of particulate material to the coastal zone (Yu et al., 2015). Moreover, the transport of riverine Fe and DOM into the Baltic has increased in recent decades as a consequence of *brownification* (Kritzberg et al., 2014), related primarily to the recovery of boreal freshwater systems from industrial acidification in the mid-20th century (Monteith et al., 2007). These changes may be expected to influence both the sediment composition and diagenetic processes in the sediments at our study sites through time. The most pronounced effect of recent coastal eutrophication on sediment chemistry has been to increase the flux of autochthonous organic matter to the sediments. Due to the consumption of electron acceptors in organic matter remineralization, carbon loading has led to a vertical migration of the redox zones of the sediments, including the SMTZ (Slomp et al., 2013; Egger et al., 2015a). Evidence for an upwards shift of the SMTZ can be seen in the total sulfur (S) contents of the sediments at stations A, D and J (Fig. 6), each of which show a distinct peak in the post-1970 sediments, close to the current position of the SMTZ. This is consistent with the time-dependent modeling simulations of Rooze at al. (2016), in which rates of FeS and FeS_2 precipitation in the SMTZ were shown to increase in response to carbon loading in the late 20th century.

A distinct interval of elevated sedimentary Fe contents can be seen at station A, centered on the early 1970s (Fig. 6). Total Fe contents in this layer are up to 3 times higher than at the present day (3% vs. 1%), indicating a dramatically increased input of Fe. No corresponding peak is observed in C_{org}, suggesting that the Fe profile cannot be explained by a simple increase in DOM input to the estuary at this time, leading to enhanced rates of flocculation and sedimentation. Nevertheless, the Fe in this interval is predominantly in the form of organic-Fe (II) complexes (Fig. 6), indicating flocculation as the likely mechanism for sedimentation of Fe. This implies that the Fe/C ratio of the riverine DOM was elevated at this time due to a secular increase in the input of Fe to the river water from an anthropogenic source, possibly the nearby blast furnace at Åminnefors (Fig. 1a), which was active from the late 19th century until 1977.

Despite these anthropogenic impacts, the role of flocculation in determining sedimentary Fe chemistry along the Mustionjoki transect has remained largely unchanged throughout the last century. Evidence of enhanced Fe input centered on the early 1970s is restricted to station A. In contrast, stations D and J record relatively constant Fe contents throughout the sediment column (Fig. 6), implying relatively static net Fe inputs. This suggests that any recent changes in riverine Fe inputs due to brownification (Sarkkola et al., 2013; Kritzberg and Ekström, 2012) have not strongly influenced sedimentary Fe in this system. Moreover, the offshore decline in sedimentary Fe contents observed in the modern surface sediments (Fig. 4b) is reproduced in the systematic decrease in Fe contents from station A–D–J observed at all depths in the sediment column (Fig. 6). Hence, on the scale of the entire transect, it can be concluded that the role of flocculation in determining the Fe distribution in these estuarine sediments has not been significantly influenced by human activities over the last century.

Biogeosciences Discuss., doi:10.5194/bg-2017-181, 2017
Manuscript under review for journal Biogeosciences
Discussion started: 19 May 2017

5.6 The spatial extent of the flocculation signal in sediment Fe chemistry

Our data confirm that estuarine sediments may trap large amounts of the Fe transported to the boreal coastal zone via rivers. When the additional surface sediment data from the Paimionjoki transect are plotted together with those from the Mustionjoki transect, sedimentary Fe/Al ratios show an apparent logarithmic decline with distance offshore. Fe/Al provides a simple indication of the reactive Fe content of sediments (Lyons and Severmann, 2006), and in this case describes the net enrichments of both organic-Fe (II) complexes and ferrihydrite, introduced to sediments as a consequence of flocculation. The absence of extreme Fe enrichments in the Paimionjoki transect is likely due to the absence of stations close to the river mouth, where organic-Fe (II) complexes are expected to accumulate, and the lack of a pronounced bathymetric sill, which limits the redox shuttling effects on ferrihydrite observed in the Mustionjoki estuary. However, Fe/Al along the Paimionjoki transect alone shows a steady decline from Fe/Al = 0.93 to Fe/Al = 0.73 over >80 km S from the river mouth (Fig. 8). Furthermore, typical Fe/Al values for oxic shelf areas of the northern Baltic Proper – several hundred km offshore – are ~0.5–0.6 (e.g., Lenz et al., 2015), implying an ongoing decline in Fe/Al offshore from station Q, our most distal sampling point. Taken together, these results suggest that the spatial signal of flocculation in sedimentary Fe chemistry in the brackish Baltic Sea is detectable over a large distance (>100 km) from the coastline. This conclusion is supported by our suspended Fe_{part} data, which shows a background of ~0.5 μmol L^{-1} Fe_{part} in the water column of station K in the open Gulf of Finland (Fig. 2). Hence, although flocculation itself likely occurs further upstream at the contact between fresh and brackish water masses, a fraction of the suspended Fe_{part} apparently evades settling in the estuarine environment and is transported offshore before sedimentation.

Considering the boreal coastal zone more broadly, the spatial impact of flocculation on sedimentary Fe chemistry is likely determined by the steepness of the offshore salinity gradient and the magnitude of the riverine Fe input. The Baltic Sea is characterized by a nearly 2000 km-long N–S surface-water salinity gradient of ~2–15, from the Bothnian Bay to the Danish Straits (Leppäranta and Myrberg, 2009). In the lowest-salinity regions in the Bothnian Bay and Bothnian Sea, the potential zone of estuarine flocculation extends further offshore and the trapping of Fe in estuarine sediments may be expected to be less efficient. At the same time, riverine Fe inputs in this region are higher than elsewhere in the Baltic Sea (Asmala et al., 2014), due to the significant release of Fe from peatlands in the catchment areas (Kortelainen et al., 2006) and the potential release of Fe from acid-sulfate soils Boman et al., 2010). Due to this combination of factors, flocculated $Fe_{part.}$ is likely dispersed over a much larger area in the Bothnian Bay and Bothnian Sea with respect to the Baltic Proper, which could explain the consistently high sedimentary Fe contents in the offshore areas of the Bothnian Sea (Slomp et al., 2013). At the other end of the spectrum, in boreal estuaries draining into fully marine systems such as in the Arctic (e.g., Dai and Martin, 1995), steeper salinity gradients likely limit the dispersion of flocculated material to a relatively narrow zone close to the river mouths.

Biogeosciences Discuss., doi:10.5194/bg-2017-181, 2017
Manuscript under review for journal Biogeosciences
Discussion started: 19 May 2017

6 Conclusions

In boreal estuaries, salinity-mediated flocculation of DOM and associated Fe strongly influences the chemistry of the sediments. We can draw the following main conclusions from the study:

- Flocculation is reflected in non-conservative mixing of $Fe_{diss.}$ along the estuarine salinity gradient. $Fe_{diss.}$ is preferentially removed from solution with increasing salinity.
- The POM generated by flocculation of DOM can be detected in suspended particulate matter using $\delta^{13}C$ and N/C of DOM as end-member reference values. Due to the presence of phytoplankton material in surface waters, flocculated OM is primarily detected in deeper waters.
- The true zone of flocculation can be identified using parallel measurements of Fe_{diss} and Fe_{part}, and occurs at low salinities, close to the primary contact between fresh and saline water masses. In the Mustionjoki estuary, this zone corresponds to the halocline of the stratified inner basin, which is laterally mobile during the seasonal cycle.
- The impacts of flocculation on sediment chemistry are most pronounced in the upper estuarine zone, where the halocline intersects the sediment-water interface. However, flocculated material accumulates in progressively lower concentrations up to tens or hundreds of kilometers offshore. The spatial scale of the flocculation signal in sediment chemistry is likely dependent on the steepness of the salinity gradient, with greater dispersal in low-salinity systems.
- Flocculation transfers POM of terrestrial origin, likely humic materials, from the water column to the sediments. The contribution of this material to sedimentary OM declines offshore as indicated by $\delta^{13}C$ and N/C of sedimentary OM.
- Flocculation transfers Fe to the sediments in two principal forms: organic-Fe (III) complexes and ferrihydrite. In sediments, Fe in organic-Fe (III)-complexes is reduced *in situ*, producing organic-Fe (II) complexes which are preserved during burial. In contrast, ferrihydrite takes part in sedimentary diagenetic reactions, influencing the pore water and sediment chemistry.
- Organic-Fe (II)-complexes in sediments are strongly concentrated close to river mouths. Ferrihydrite in sediments is also more concentrated in upper estuarine regions, but due to redox shuttling effects may be redistributed from the original site of sedimentation.
- The impact of flocculation on sediment chemistry is modulated by the gradient of bottom water sulfate concentrations along the estuarine salinity gradient. Opposing gradients of Fe and sulfate availability for diagenetic reactions are observed with increasing distance offshore. These impact on the vertical zonation of sediment biogeochemistry, most markedly in determining the depth of the SMTZ and the accumulation of hydrogen sulfide and Fe^{2+} in pore waters.

- Although Fe and DOM inputs to boreal estuaries have been shown to be increasing over recent decades due to brownification, Fe inputs to sediments in our principal study transect remained largely constant over the same interval. However, coastal eutrophication has had a strong impact on sediment chemistry through increased carbon inputs, leading to a shoaling of the SMTZ and increased rates of the associated sedimentary reactions.

Data availability

All data from Figures 1–8 of the manuscript and Supplementary Figure 1 will be made available in Pangaea upon publication of the article.

Supplement link

Supplementary Figure 1 is uploaded in parallel with the manuscript and is available from the Biogeosciences website.

Author contributions

TJ devised the study, carried out field and laboratory work, interpreted the data, produced the figures and wrote the paper. EA interpreted the data and assisted with writing the paper. CS carried out the Mössbauer analysis, interpreted the data and assisted with writing the paper. RT carried out fieldwork and sequential Fe extractions, interpreted the data, produced figures and wrote the MSc thesis which formed the basis for the paper. J-PM carried out fieldwork, analyzed methane samples and assisted with writing the paper. JV, AK and PP provided sample material, interpreted the data and assisted with writing the paper. PE assisted with ICP-OES analysis. SH managed the project which principally funded the study, carried out fieldwork, interpreted the data and assisted with writing the paper.

Competing interest statement

The authors declare no competing interest.

Acknowledgements

We acknowledge support in field campaigns from Tvärminne Zoological Station, Göran Lundberg, Veijo Kinnunen, Ari Ruuskanen, Mikael Kraft, Petra Tallberg, Anni Jylhä-Vuorio and Kaarina Lukkari. Analytical and laboratory assistance was provided by Juhani Virkanen, Antti Nevalainen, Jaana Koistinen and Asko Simojoki. This research was funded by Academy of Finland projects 139267, 272964 and 267112, Maa ja Vesitekniikan Tuki projects 31749 and 32861, and by the BONUS COCOA project (grant agreement 2112932-1), funded jointly by the EU and Danish Research Council.

References

Arndt, S., Jorgensen, B. B., LaRowe, D. E., Middelburg, J. J., Pancost, R. D. and Regnier, P.: Quantifying the degradation of organic matter in marine sediments: A review and synthesis, Earth-Sci. Rev., 123, 53-86, 10.1016/j.earscirev.2013.02.008, 2013.

Asmala, E., Autio, R., Kaartokallio, H., Pitkanen, L., Stedmon, C. A. and Thomas, D. N.: Bioavailability of riverine dissolved organic matter in three Baltic Sea estuaries and the effect of catchment land use, Biogeosciences, 10, 6969–6986, 10.5194/bg–10–6969–2013, 2013.

Asmala, E., Bowers, D. G., Autio, R., Kaartokallio, H. and Thomas, D. N.: Qualitative changes of riverine dissolved organic matter at low salinities due to flocculation, J. Geophys. Res. –Biogeosci., 119, 1919–1933, 10.1002/2014JG002722, 2014.

Asmala, E., Kaartokallio, H., Carstensen, J. and Thomas, D. N.: Variation in riverine inputs affect dissolved organic matter characteristics throughout the estuarine gradient, Front. Mar. Sci., 2, 125, 2016.

Berg, P., Risgaard–Petersen, N. and Rysgaard, S.: Interpretation of measured concentration profiles in sediment pore water, Limnol. Oceanogr., 43, 1500–1510, 1998.

Berner, R.: Sedimentary pyrite formation, Am. J. Sci., 268, 1–23, 1970.

Berner, R. and Raiswell, R.: C/S method for distinguishing fresh-water from marine sedimentary rocks, Geology, 12, 365–368, 10.1130/0091–7613(1984)12<365:CMFDFF>2.0.CO;2, 1984.

Boman, A., Frojdo, S., Backlund, K. and Astrom, M. E.: Impact of isostatic land uplift and artificial drainage on oxidation of brackish-water sediments rich in metastable iron sulfide, Geochim. Cosmochim. Acta, 74, 1268–1281, 10.1016/j.gca.2009.11.026, 2010.

Boyle, E., Edmond, J. and Sholkovitz, E.: Mechanism of iron removal in estuaries, Geochim. Cosmochim. Acta, 41, 1313–1324, 10.1016/0016–7037(77)90075–8, 1977.

Burton, E. D., Sullivan, L. A., Bush, R. T., Johnston, S. G. and Keene, A. F.: A simple and inexpensive chromium-reducible sulfur method for acid–sulfate soils, Appl. Geochem., 23, 2759–2766, 10.1016/j.apgeochem.2008.07.007, 2008.

Canfield, D. E., Kristensen, E., and Thamdrup, B.: Aquatic Geomicrobiology, Elsevier, Amsterdam, the Netherlands, 2005.

Cline, J.: Spectrophotometric determination of hydrogen sulfide in natural waters, Limnol. Oceanogr., 14, 454–&, 1969.

Conley, D. J., Carstensen, J., Aigars, J., Axe, P., Bonsdorff, E., Eremina, T., Haahti, B., Humborg, C., Jonsson, P., Kotta, J., Lannegren, C., Larsson, U., Maximov, A., Medina, M. R., Lysiak–Pastuszak, E., Remeikaite–Nikiene, N., Walve, J., Wilhelms, S. and Zillen, L.: Hypoxia is increasing in the coastal zone of the Baltic Sea, Environ. Sci. Technol., 45, 6777–6783, 10.1021/es201212r, 2011.

Dai, M. and Martin, J.: First data on trace-metal level and behavior in 2 major Arctic river-estuarine systems (Ob and Yenisey) and in the adjacent Kara Sea, Russia, Earth Planet. Sci. Lett., 131, 127–141, 10.1016/0012–821X(95)00021–4, 1995.

Dalzell, B. J., Minor, E. C. and Mopper, K. M.: Photodegradation of estuarine dissolved organic matter: a multi-method assessment of DOM transformation, Org. Geochem., 40, 243–257, 10.1016/j.orggeochem.2008.10.003, 2009.

de Leeuw, J.W., and Largeau, C.: A review of macromolecular organic compounds that comprise living organisms and their role in kerogen, coal and petroleum formation, in: Organic Geochemistry, Principles and Applications, Engel, M. H. and Macko, S.A. (Eds), Plenum Press, New York, U.S.A., 23–72, 1993.

Dzombak, D., and Morel, F. M. M.: Surface complexation modeling: Hydrous ferric oxide, Wiley, New York, U.S.A., 1990.

Eckert, J. and Sholkovitz, E.: Flocculation of iron, aluminum and humates from river water by electrolytes, Geochim. Cosmochim. Acta, 40, 847–848, 10.1016/0016–7037(76)90036–3, 1976.

Egger, M., Jilbert, T., Behrends, T., Rivard, C. and Slomp, C. P.: Vivianite is a major sink for phosphorus in methanogenic coastal surface sediments, Geochim. Cosmochim. Acta, 169, 217–235, 10.1016/j.gca.2015.09.012, 2015.

Egger, M., Kraal, P., Jilbert, T., Sulu–Gambari, F., Sapart, C. J., Rockmann, T. and Slomp, C. P.: Anaerobic oxidation of methane alters sediment records of sulfur, iron and phosphorus in the Black Sea, Biogeosciences, 13, 5333–5355, 10.5194/bg–13–5333–2016, 2016.

Egger, M., Rasigraf, O., Sapart, C. J., Jilbert, T., Jetten, M. S. M., Rockmann, T., van der Veen, C., Banda, N., Kartal, B., Ettwig, K. F. and Slomp, C. P.: Iron-mediated anaerobic oxidation of methane in brackish coastal sediments, Environ. Sci. Technol., 49, 277–283, 10.1021/es503663z, 2015.

Eusterhues, K., Wagner, F. E., Haeusler, W., Hanzlik, M., Knicker, H., Totsche, K. U., Koegel–Knabner, I. and Schwertmann, U.: Characterization of ferrihydrite-soil organic matter coprecipitates by X-ray Diffraction and Mössbauer spectroscopy, Environ. Sci. Technol., 42, 7891–7897, 10.1021/es800881w, 2008.

Forsgren, G., Jansson, M. and Nilsson, P.: Aggregation and sedimentation of iron, phosphorus and organic carbon in experimental mixtures of freshwater and estuarine water, Estuar. Coast. Shelf Sci., 43, 259–268, 10.1006/ecss.1996.0068, 1996.

Geyer, W.: The importance of suppression of turbulence by stratification on the estuarine turbidity maximum, Estuaries, 16, 113–125, 10.2307/1352769, 1993.

Goñi, M., Teixeira, M. and Perkey, D.: Sources and distribution of organic matter in a river-dominated estuary (Winyah Bay, SC, USA), Estuar. Coast. Shelf Sci., 57, 1023–1048, 10.1016/S0272–7714(03)00008–8, 2003.

Hausen, H.: Ytgestaltningen i Åbolands–Ålands skärgård och dess orsaker, in: Skärgårdsboken, Nordenskiöld-samfundet i Finland, Helsinki, Finland, 30–73, 1948 (in Swedish).

Hedges, J., Mayorga, E., Tsamakis, E., McClain, M., Aufdenkampe, A., Quay, P., Richey, J., Benner, R., Opsahl, S., Black, B., Pimentel, T., Quintanilla, J. and Maurice, L.: Organic matter in Bolivian tributaries of the Amazon River: A comparison to the lower mainstream, Limnol. Oceanogr., 45, 1449–1466, 2000.

Ingri, J., and Conrad, S.: Distinct iron isotope signatures in suspended matter in the northern Baltic Sea; implications for cycling of organic carbon and phosphorus, EGU General Assembly, Vienna, Austria, 12–17 April 2015, EGU2015–11738, 2015.

James, F.: MINUIT Tutorial – Function Minimization, in: Proceedings of the 1972 CERN computing and data processing school, Pertisau, Austria, 10–24 September, 1972, CERN, Switzerland, 72–21, http://seal.web.cern.ch/seal/documents/minuit/mntutorial.pdf, 2004.

Jilbert, T. and Slomp, C. P.: Iron and manganese shuttles control the formation of authigenic phosphorus minerals in the euxinic basins of the Baltic Sea, Geochim. Cosmochim. Acta, 107, 155–169, 10.1016/j.gca.2013.01.005, 2013.

Klingelhöfer, G., Morris, R. V., Bernhardt, B., Rodionov, D., de Souza Jr., P. A., Squyres, S. W., Foh, J., Kankeleit, E., Bonnes, U., Gellert, R., Schröder, C., Linkin, S., Evlanov, E., Zubkov, B., and Prilutski, O.: Athena MIMOS II Mössbauer spectrometer investigation. J. Geophys. Res. 108, E12, 8067, http://dx.doi.org/10.1029/2003JE002138, 2003.

Kortelainen, P., Mattsson, T., Finer, L., Ahtiainen, M., Saukkonen, S. and Sallantaus, T.: Controls on the export of C, N, P and Fe from undisturbed boreal catchments, Finland, Aquat. Sci., 68, 453–468, 10.1007/s00027–006–0833–6, 2006.

Kraal, P., Burton, E. D., Rose, A. L., Kocar, B. D., Lockhart, R. S., Grice, K., Bush, R. T., Tan, E. and Webb, S. M.: Sedimentary iron-phosphorus cycling under contrasting redox conditions in a eutrophic estuary, Chem. Geol., 392, 19–31, 10.1016/j.chemgeo.2014.11.006, 2015.

Krachler, R., Krachler, R. F., Wallner, G., Steier, P., El Abiead, Y., Wiesinger, H., Jirsa, F. and Keppler, B. K.: Sphagnum–dominated bog systems are highly effective yet variable sources of bio-available iron to marine waters, Sci. Total Environ., 556, 53–62, 10.1016/j.scitotenv.2016.03.012, 2016.

Kritzberg, E. S. and Ekstrom, S. M.: Increasing iron concentrations in surface waters – a factor behind brownification?, Biogeosciences, 9, 1465–1478, 10.5194/bg–9–1465–2012, 2012.

Kritzberg, E. S., Villanueva, A. B., Jung, M. and Reader, H. E.: Importance of boreal rivers in providing iron to marine waters, PLoS One, 9, e107500, 10.1371/journal.pone.0107500, 2014.

Lahermo, P., Väänänen, P., Tarvainen, T. and Salminen, R.: Geochemical Atlas of Finland Part 3: Environmental Geochemistry – stream waters and sediments, Geological Survey of Finland, Espoo, Finland, 1996.

Lalonde, K., Mucci, A., Ouellet, A. and Gélinas, Y.: Preservation of organic matter in sediments promoted by iron, Nature, 483, 198–200, 2012.

Lenz, C., Jilbert, T., Conley, D. J. and Slomp, C. P.: Hypoxia-driven variations in iron and manganese shuttling in the Baltic Sea over the past 8 kyr, Geochem. Geophys. Geosyst., 16, 3754–3766, 10.1002/2015GC005960, 2015.

Leppäranta, M., and Myrberg, K.: Physical Oceanography of the Baltic Sea, Springer-Praxis, Heidelberg, Germany, 2009.

Li, C., Yang, S., Lian, E., Wang, Q., Fan, D. and Huang, X.: Chemical speciation of iron in sediments from the Changjiang Estuary and East China Sea: Iron cycle and paleoenvironmental implications, Quatern. Int., http://dx.doi.org/10.1016/j.quaint.2016.07.014, in press.

Lisitsyn, A. P.: The marginal filter of the ocean, Oceanology 34, 671–68, 1995.

Lovley, D., Holmes, D. and Nevin, K.: Dissimilatory Fe(III) and Mn(IV) reduction, Advances in Microbial Physiology, 49, 219–286, 10.1016/S0065–2911(04)49005–5, 2004.

Lyons, T. W. and Severmann, S.: A critical look at iron paleoredox proxies: New insights from modern euxinic marine basins, Geochim. Cosmochim. Acta, 70, 5698–5722, 10.1016/j.gca.2006.08.021, 2006.

Monteith, D. T., Stoddard, J. L., Evans, C. D., de Wit, H. A., Forsius, M., Hogasen, T., Wilander, A., Skjelkvale, B. L., Jeffries, D. S., Vuorenmaa, J., Keller, B., Kopacek, J. and Vesely, J.: Dissolved organic carbon trends resulting from changes in atmospheric deposition chemistry, Nature, 450, 537-U9, 10.1038/nature06316, 2007.

Moran, M., Sheldon, W. and Zepp, R.: Carbon loss and optical property changes during long–term photochemical and biological degradation of estuarine dissolved organic matter, Limnol. Oceanogr., 45, 1254–1264, 2000.

Neubauer, E., Kohler, S. J., von der Kammer, F., Laudon, H. and Hofmann, T.: Effect of pH and stream order on iron and arsenic speciation in boreal catchments, Environ. Sci. Technol., 47, 7120–7128, 10.1021/es401193j, 2013.

Niemi, Å.: Hydrography and oxygen fluctuations in Pojoviken, southern coast of Finland, 1972–1975. Meri 4, 23–35, 1977.

Norkko, J., Reed, D. C., Timmermann, K., Norkko, A., Gustafsson, B. G., Bonsdorff, E., Slomp, C. P., Carstensen, J. and Conley, D. J.: A welcome can of worms? Hypoxia mitigation by an invasive species, Global Change Biol., 18, 422–434, 10.1111/j.1365–2486.2011.02513.x, 2012.

Officer, C. B.: Physical oceanography of estuaries, Wiley, New York, U.S.A., 1976.

O'Sullivan, T. D., and Smith, N.O.: The solubility and partial molar volume of nitrogen and methane in water and in aqueous sodium chloride from 50 to 125'C and 100 to 600 atm, J. Phys. Chem., 74, 1460–1466, 1970.

Peltola, P., Virtasalo, J. J., Oberg, T. and Astrom, M.: Geochemistry of surface sediments in the Archipelago Sea, SW Finland: a multiparameter and multivariate study, Environ. Earth Sci., 62, 725–734, 10.1007/s12665–010–0561–z, 2011.

Poulton, S. and Canfield, D.: Development of a sequential extraction procedure for iron: implications for iron partitioning in continentally derived particulates, Chem. Geol., 214, 209–221, 10.1016/j.chemgeo.2004.09.003, 2005.

Poulton, S. and Raiswell, R.: The low-temperature geochemical cycle of iron: From continental fluxes to marine sediment deposition, Am. J. Sci., 302, 774–805, 10.2475/ajs.302.9.774, 2002.

Raiswell, R. and Anderson, T.: Reactive iron enrichment in sediments deposited beneath euxinic bottom waters: constraints on supply by shelf recycling, Geol. Soc. Spec. Publ., 248, 179–194, 10.1144/GSL.SP.2005.248.01.10, 2005.

Raiswell, R.: Iron transport from the continents to the open ocean: The aging–rejuvenation cycle, Elements, 7, 101–106, 10.2113/gselements.7.2.101, 2011.

Reed, D. C., Slomp, C. P. and Gustafsson, B. G.: Sedimentary phosphorus dynamics and the evolution of bottom–water hypoxia: A coupled benthic-pelagic model of a coastal system, Limnol. Oceanogr., 56, 1075–1092, 10.4319/lo.2011.56.3.1075, 2011.

Reese, B. K., Finneran, D. W., Mills, H. J., Zhu, M. and Morse, J. W.: Examination and refinement of the determination of aqueous hydrogen sulfide by the methylene blue method, Aquat. Geochem., 17, 567–582, 10.1007/s10498–011–9128–1, 2011.

Renberg, I., Bindler, R. and Brannvall, M. L.: Using the historical atmospheric lead–deposition record as a chronological marker in sediment deposits in Europe, Holocene, 11, 511–516, 2001.

Robertson, E. K., Roberts, K. L., Burdorf, L. D. W., Cook, P., and Thamdrup, B.: Dissimilatory nitrate reduction to ammonium coupled to Fe (II) oxidation in sediments of a periodically hypoxic estuary. Limnol. Oceanogr. 61, 365–381, 2016.

Rooze, J., Egger, M., Tsandev, I. and Slomp, C. P.: Iron-dependent anaerobic oxidation of methane in coastal surface sediments: Potential controls and impact, Limnol. Oceanogr., 61, S267–S282, 10.1002/lno.10275, 2016.

Sanford, L., Suttles, S. and Halka, J.: Reconsidering the physics of the Chesapeake Bay estuarine turbidity maximum, Estuaries, 24, 655–669, 10.2307/1352874, 2001.

Sarkkola, S., Nieminen, M., Koivusalo, H., Lauren, A., Kortelainen, P., Mattsson, T., Palviainen, M., Piirainen, S., Starr, M. and Finer, L.: Iron concentrations are increasing in surface waters from forested headwater catchments in eastern Finland, Sci. Total Environ., 463, 683–689, 10.1016/j.scitotenv.2013.06.072, 2013.

Schwertmann, U. and Taylor, R.M., Iron oxides, in: Minerals in Soil Environments, Dixon, J. B., Weed, S. B., Kittrick, J. A., Milford, M. H. and White, J. L. (Eds), Soil Science Society of America, Madison, Wisconsin, U.S.A., 145–180, 1977.

Schwertmann, U., Stanjek, H. and Becher, H.: Long–term in vitro transformation of 2-line ferrihydrite to goethite/hematite at 4, 10, 15 and 25 degrees C, Clay Miner., 39, 433–438, 10.1180/0009855043940145, 2004.

Shields, M. R., Bianchi, T. S., Gelinas, Y., Allison, M. A. and Twilley, R. R.: Enhanced terrestrial carbon preservation promoted by reactive iron in deltaic sediments, Geophys. Res. Lett., 43, 1149–1157, 10.1002/2015GL067388, 2016.

Sholkovitz, E., Boyle, E. and Price, N.: Removal of dissolved humic acids and iron during estuarine mixing, Earth Planet. Sci. Lett., 40, 130–136, 10.1016/0012–821X(78)90082–1, 1978.

Sivan, O., Adler, M., Pearson, A., Gelman, F., Bar–Or, I., John, S. G. and Eckert, W.: Geochemical evidence for iron–mediated anaerobic oxidation of methane, Limnol. Oceanogr., 56, 1536–1544, 10.4319/lo.2011.56.4.1536, 2011.

Slomp, C. P., Mort, H. P., Jilbert, T., Reed, D. C., Gustafsson, B. G. and Wolthers, M.: Coupled dynamics of iron and phosphorus in sediments of an oligotrophic coastal basin and the impact of anaerobic oxidation of methane, PLoS ONE, 8, e62386, 10.1371/journal.pone.0062386, 2013.

Slomp, C. P., Epping, E. H. G., Helder, W. and Van Raaphorst, W.: A key role for iron-bound phosphorus in authigenic apatite formation in North Atlantic continental platform sediments, J. Mar. Res., 54, 1179–1205, 1996.

Slomp, C., Van der Gaast, S. and Van Raaphorst, W.: Phosphorus binding by poorly crystalline iron oxides in North Sea sediments, Mar. Chem., 52, 55–73, 10.1016/0304–4203(95)00078–X, 1996.

Stolpe, B. and Hassellov, M.: Changes in size distribution of fresh water nanoscale colloidal matter and associated elements on mixing with seawater, Geochim. Cosmochim. Acta, 71, 3292–3301, 10.1016/j.gca.2007.04.025, 2007.

Sundman, A., Karlsson, T., Laudon, H. and Persson, P.: XAS study of iron speciation in soils and waters from a boreal catchment, Chem. Geol., 364, 93–102, 10.1016/j.chemgeo.2013.11.023, 2014.

Syvitski, J. and Murray, J.: Particle Interaction in fjord suspended sediment, Mar. Geol., 39, 215–242, 10.1016/0025–3227(81)90073–6, 1981.

Uher, G., Hughes, C., Henry, G. and Upstill–Goddard, R.: Non–conservative mixing behavior of colored dissolved organic matter in a humic-rich, turbid estuary, Geophys. Res. Lett., 28, 3309–3312, 10.1029/2000GL012509, 2001.

Virta, J.: Estimating the water and salt budgets of a stratified estuary, Nord. Hydrol., 8, 11–32, 1977.

Virtasalo, J. J., and Kotilainen, A. T.: Phosphorus forms and reactive iron in late glacial, postglacial and brackish-water sediments of the Archipelago Sea, northern Baltic Sea. Mar. Geol., 252, 1–12, 2008.

Virtasalo, J., Kohonen, T., Vuorinen, I. and Huttula, T.: Sea bottom anoxia in the Archipelago Sea, northern Baltic Sea – Implications for phosphorus remineralization at the sediment surface, Mar. Geol., 224, 103–122, 10.1016/j.margeo.2005.07.010, 2005.

Virtasalo, J. J., Kotilainen, A. T., Räsänen, M. E., and Ojala, A. E. K.: Late-glacial and post–glacial deposition in a large, low relief, epicontinental basin: the northern Baltic Sea, Sedimentology, 54, 1323–1344, 2007.

Voipio, A.: The Baltic Sea, Elsevier, Amsterdam, The Netherlands, 1981.

Winterhalter, B., Flodén, T., Ignatius, H., Axberg, S., and Niemistö, L.: Geology of the Baltic Sea, in: The Baltic Sea, Voipio, A. (Ed), Elsevier, Amsterdam, The Netherlands, 1981.

Yu, C., Virtasalo, J. J., Karlsson, T., Peltola, P., Osterholm, P., Burton, E. D., Arppe, L., Hogmalm, J. K., Ojala, A. E. K. and Astrom, M. E.: Iron behavior in a northern estuary: Large pools of non-sulfidized Fe(II) associated with organic matter, Chem. Geol., 413, 73–85, 10.1016/j.chemgeo.2015.08.013, 2015.

Zillen, L., Lenz, C. and Jilbert, T.: Stable lead (Pb) isotopes and concentrations – A useful independent dating tool for Baltic Sea sediments, Quat. Geochronol., 8, 41–45, 10.1016/j.quageo.2011.11.001, 2012.

Biogeosciences Discuss., doi:10.5194/bg-2017-181, 2017
Manuscript under review for journal Biogeosciences
Discussion started: 19 May 2017

Tables

Campaign and Station code	Co-ordinates (degree-decimal) °N	°E	Water depth (m, sediment stations only)	Water sampling	Sediment sampling
Mustionjoki transect September 2014; June 2015					
A	60.091617	23.554630	7	Full profile (2015)	4 samples (2014) Full profile (2015)
B	60.079833	23.531167	11	Full profile (2015)	5 samples (2014)
C	60.054300	23.509517	22	Full profile (2015)	5 samples (2014)
D	60.022650	23.474600	39	Full profile (2015)	5 samples (2014) Full profile (2015)
E	60.014033	23.467950	21	Full profile (2015)	5 samples (2014)
F	59.994750	23.452300	8	Full profile (2015)	5 samples (2014)
G	59.961383	23.396730	6	Full profile (2015)	5 samples (2014)
H	59.920117	23.332650	17	Full profile (2015)	5 samples (2014)
I	59.907367	23.326200	21	Full profile (2015)	5 samples (2014)
J	59.855286	23.261780	33	Full profile (2015)	5 samples (2014) Full profile (2015)
K	59.789867	23.335430	47	Full profile (2015)	5 samples (2014)
Paimionjoki transect August-September 2001					
L	60.354667	22.563000	18		Surface (0–2 cm)
M	60.313333	22.509833	46		Surface (0–2 cm)
N	60.140970	22.410722	27		Surface (0–2 cm)
O	60.057288	22.355018	46		Surface (0–2 cm)
P	59.913438	21.753072	35		Surface (0–2 cm)
Q	59.764387	21.706720	107		Surface (0–2 cm)
Mustionjoki transect April-August-October 2011					
a	60.095467	23.590867		Surface only	
b	60.036650	23.484183		Surface only	
c	59.977800	23.421300		Surface only	
d	59.917300	23.324433		Surface only	
e	59.855567	23.261967		Surface only	
f	59.816317	23.271450		Surface only	

Table 1. Sampling campaigns and stations (see also Fig. 1).

Biogeosciences Discuss., doi:10.5194/bg-2017-181, 2017
Manuscript under review for journal Biogeosciences
Discussion started: 19 May 2017

Extraction stage	Reagent	Nominal target phases (original protocol)	Interpreted phases (this study)
1	Na acetate, pH 4.5, 24 h	Fe-carbonates (siderite, ankerite)	Ferrihydrite
2	Hydroxylamine-HCl, 48 h	Poorly crystalline Fe oxides (ferrihydrite, lepidocrocite)	Ferrihydrite
3	Na dithionite, 2 h	Crystalline Fe oxides (goethite, akaganéite, hematite)	Organic Fe (II) complexes
4	Ammonium oxalate, 6 h	Magnetite	Organic Fe (II) complexes, magnetite
5	HCl, 12 M, boiling	Reactive sheet-silicate Fe	Reactive sheet-silicate Fe
6 (sulfide-Fe)	Total digestion + ICP-OES analysis for S		Pyrite
Total Fe	Total digestion + ICP-OES analysis for Fe		All Fe phases in sample
7 Residual Fe	Calculated (Total Fe – Σ[1-6])	Unreactive silicate Fe	Unreactive silicate Fe

Table 2. Stages of the sequential extraction for Fe used in this study, based on the protocol of Poulton and Canfield (2005).

Biogeosciences Discuss., doi:10.5194/bg-2017-181, 2017
Manuscript under review for journal Biogeosciences
Discussion started: 19 May 2017

Mineral Phase	δ^a (mm/s)	$\Delta_{EQ}{}^b$ (mm/s)	$B_{hf}{}^c$ (T)	Area^d (%)
Station A				
Magnetite $Fe^{2.5+}$	[0.67]^e	[0.00]	[46.5]	9
Magnetite Fe^{3+}	[0.30]	[0.03]	[49.8]	5
Silicate Fe^{2+}	1.08	2.61	-	18
Undocumented Fe^{2+} ("organic-Fe (II)")	0.78	0.83	-	42
Superparamagn. FeOx Fe^{3+} ("ferrihydrite")	0.32	0.67	-	26
Station D				
Silicate Fe^{2+}	1.19	2.48	-	49
Superparamagn. FeOx Fe^{3+} ("ferrihydrite")	0.25	0.86	-	51

[a]Isomer or center shift.

[b]Quadrupole splitting.

[c]Internal magnetic field.

[d]Suspectral area ratio, to first order proportional to relative amount of total Fe contained in mineral phase. A general uncertainty of ±2% absolute is applied.

[e]Values in square brackets were fixed to values from library spectra during the fitting process.

Table 3. Mössbauer parameters corresponding to spectra in Fig. 5.

Biogeosciences Discuss., doi:10.5194/bg-2017-181, 2017
Manuscript under review for journal Biogeosciences
Discussion started: 19 May 2017

Figures

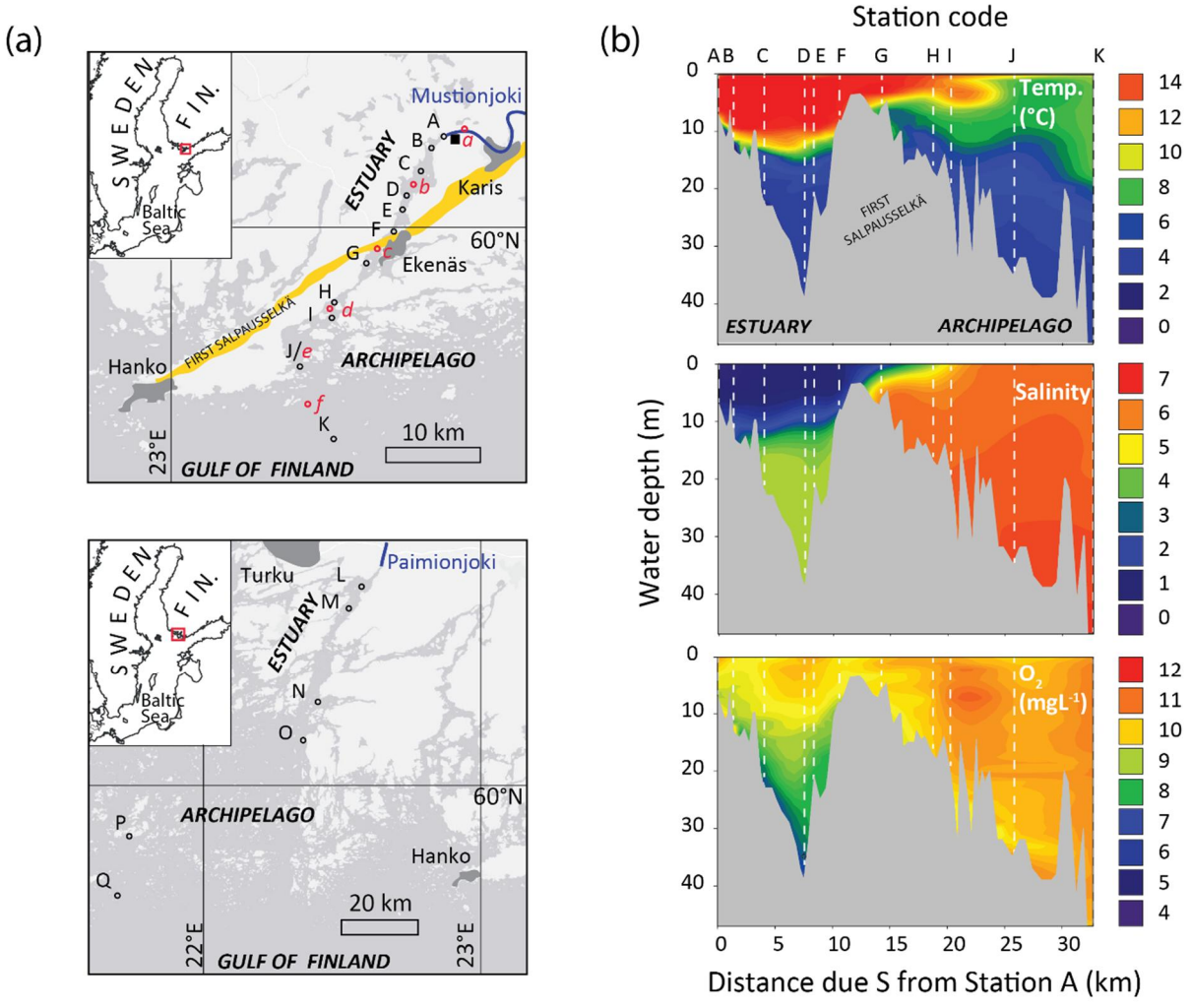

Figure 1. (a) Location of the Mustionjoki estuary transect (top) and the Paimionjoki estuary transect (bottom). In both systems, point-source river inputs discharge into a channel-like estuary, which in turn connects into the archipelago coastline of the Gulf of Finland, northern Baltic Sea. Sediment and water column sampling locations are indicated A–Q. Dissolved organic matter (DOM) sampling locations (Asmala et al 2014, 2016) are indicated *a-f*. The location of the Åminnefors blast furnace is indicated by the black square. The First Salpausselkä ice-marginal formation is indicated in yellow. (b) Water column characteristics of the Mustionjoki transect during sampling in June 2015. 2D contour plots were generated by extrapolation between the measured profiles at stations A–K using Sigmaplot™ software. Distances along transect are reported as distance directly due S from Station A at the Mustionjoki river mouth.

Biogeosciences Discuss., doi:10.5194/bg-2017-181, 2017
Manuscript under review for journal Biogeosciences
Discussion started: 19 May 2017

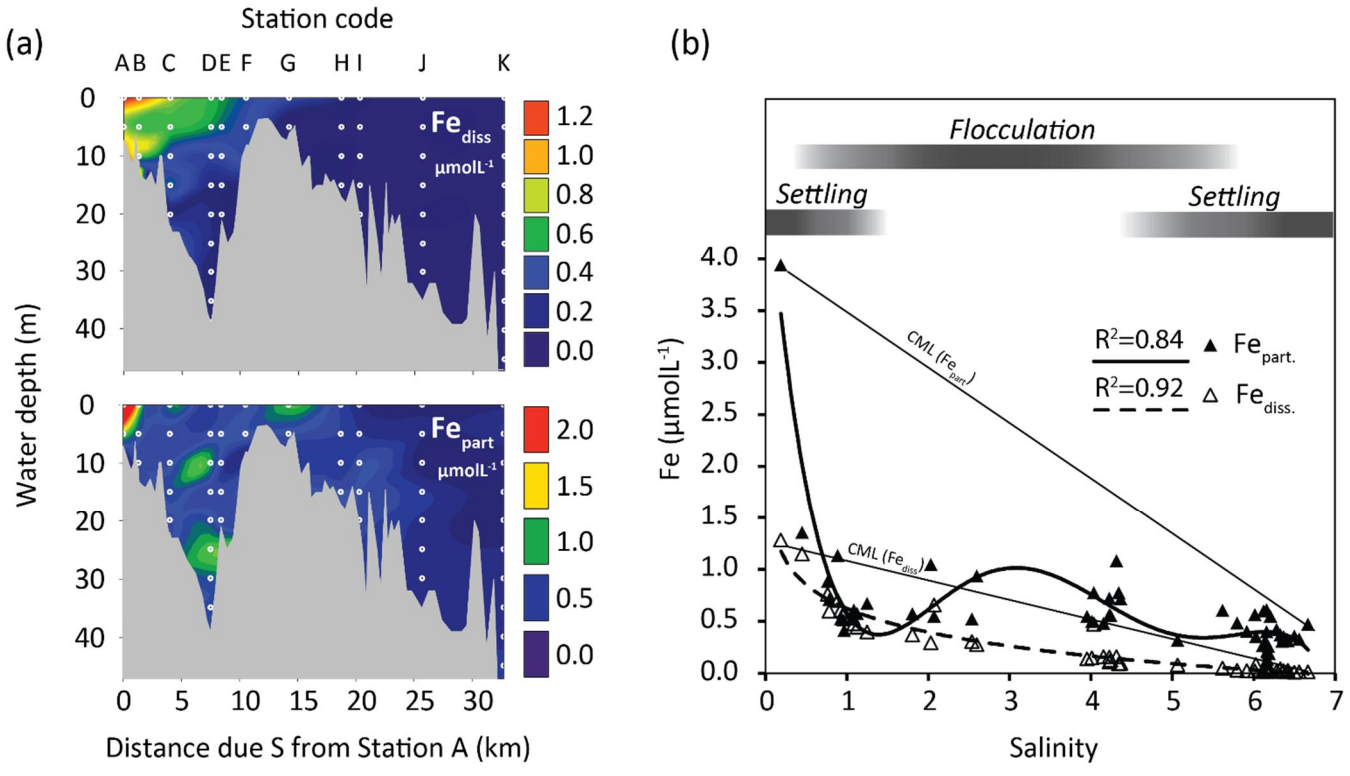

Figure 2. (a) 2D contour plots of dissolved (top) and particulate (bottom) Fe in the water column along the Mustionjoki transect (Stations A–K), operationally defined by filtration at 0.45 µm, June 2015. White circles represent sampling positions (vertical depth resolution = 5m). (b) Data from *a* plotted against salinity, including trendlines for $Fe_{part.}$ (polynomial) and $Fe_{diss.}$ (logarithmic). Linear Conservative Mixing Lines (CML) are drawn between the high- and low-salinity end-member samples for Fe_{part} and Fe_{diss}. The inferred dominant processes controlling Fe_{part} along the salinity transect are indicated by the grey bars.

Biogeosciences Discuss., doi:10.5194/bg-2017-181, 2017
Manuscript under review for journal Biogeosciences
Discussion started: 19 May 2017

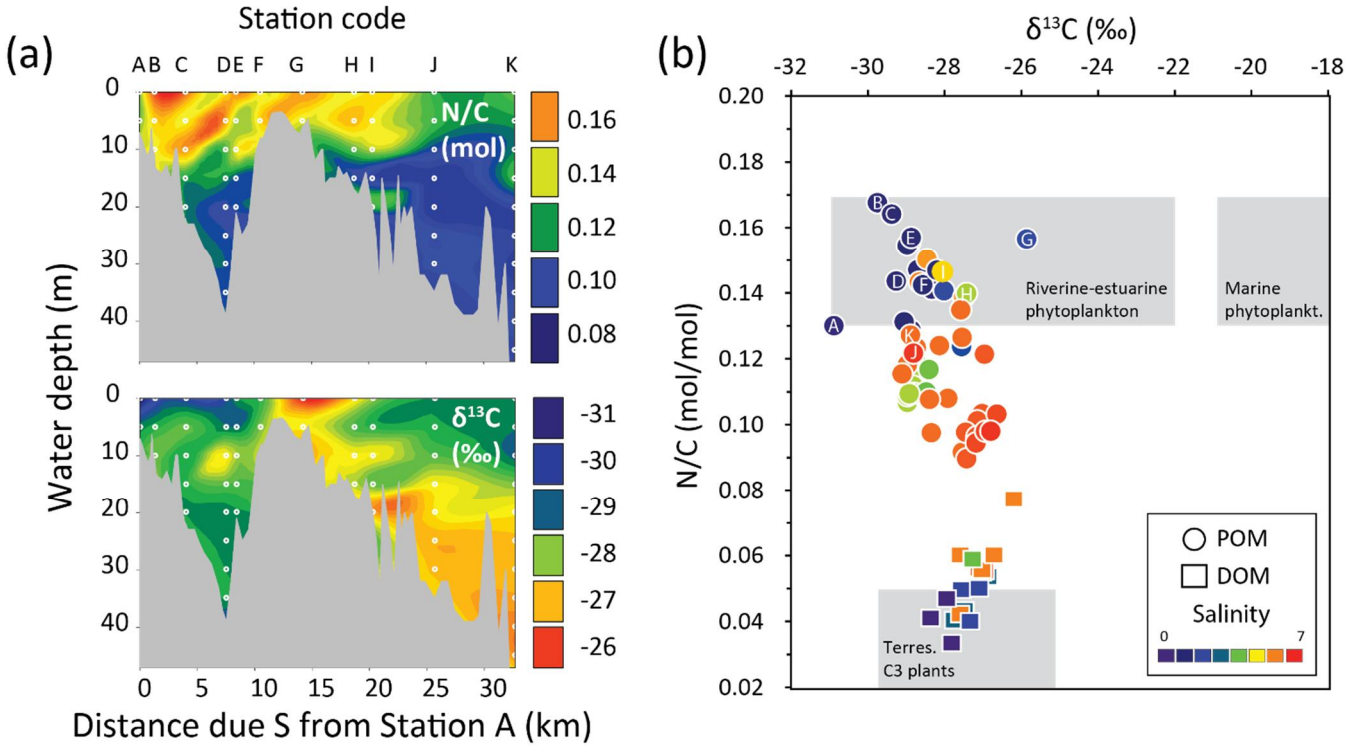

Figure 3. (a) 2D contour plots of molar N/C (top) and $\delta^{13}C$ (bottom) of particulate organic matter (POM) along the Mustionjoki transect, operationally defined by filtration at 0.45 µm, June 2015. White circles represent sampling positions (vertical depth resolution = 5m). (b) Cross plot of molar N/C vs. $\delta^{13}C$ of POM in June 2015 (circles, each representing a single sample from the 2D plot in *a*) and of published data for dissolved organic matter (DOM) from the same transect (squares, surface water only, 6 samples each from campaigns in April, August and October 2011). In-situ salinity at the time and location of sampling is indicated by the color scale. Samples marked with letters indicate surface water samples. Organic matter source fields are taken from Goñi et al. (2003).

Biogeosciences Discuss., doi:10.5194/bg-2017-181, 2017
Manuscript under review for journal Biogeosciences
Discussion started: 19 May 2017

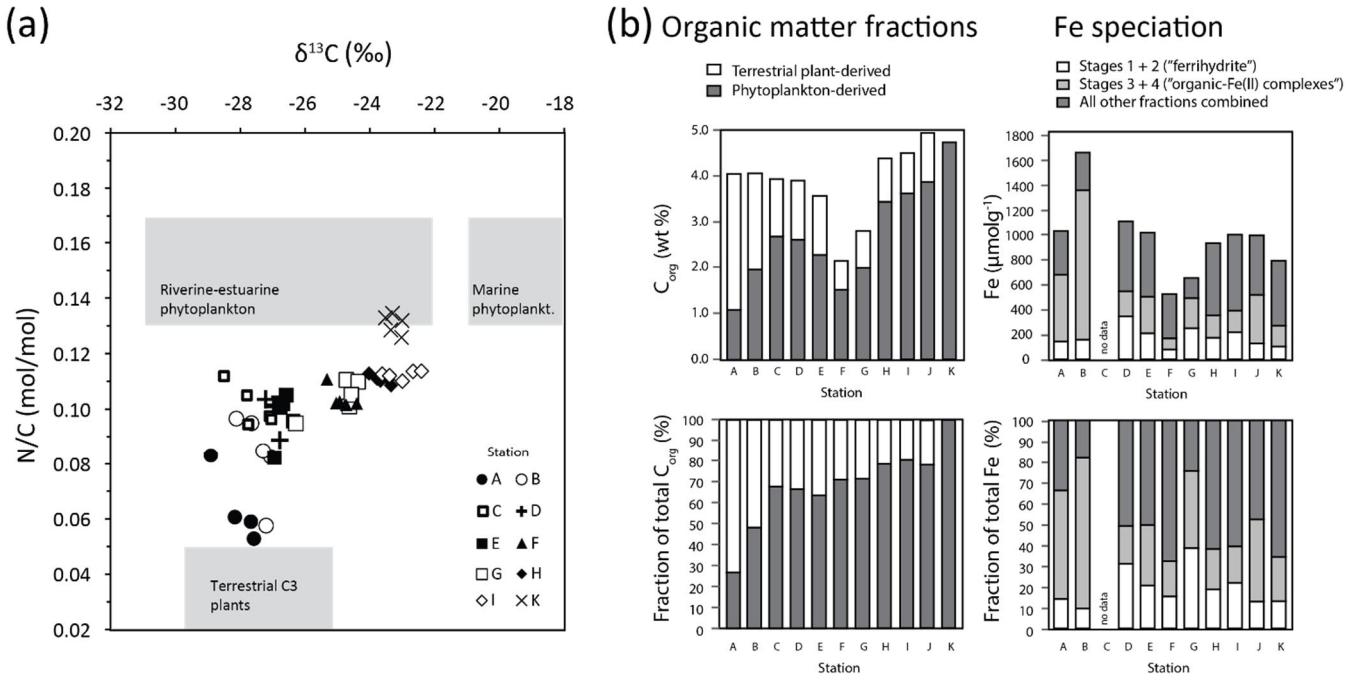

Figure 4. (a) Cross plot of molar N/C vs. $\delta^{13}C$ of sedimentary organic matter along the Mustionjoki transect. Stations are indicated by the symbols. No isotope data was available for station J. Four or five samples are plotted for each station, representing evenly spaced 2 cm thick slices throughout a GEMAX™ core of 30–60 cm length (e.g. Station K: 0–2 cm; 8.5–10.5 cm, 17–19 cm, 25.5–27.5 cm, 34–36 cm). (b) Organic matter fractions of the same sediment samples, derived from molar N/C ratios, assuming end-member values of N/C = 0.04 (terrestrial-derived) and 0.13 (phytoplankton-derived). Mean values are reported of the 4 or 5 samples from each core; Operational Fe speciation of surface-sediment samples (0–2 cm), derived from sequential extraction by the method of Poulton and Canfield (2005) and an additional extraction for sulfide-bound Fe. No extraction data was available for station C.

Biogeosciences Discuss., doi:10.5194/bg-2017-181, 2017
Manuscript under review for journal Biogeosciences
Discussion started: 19 May 2017

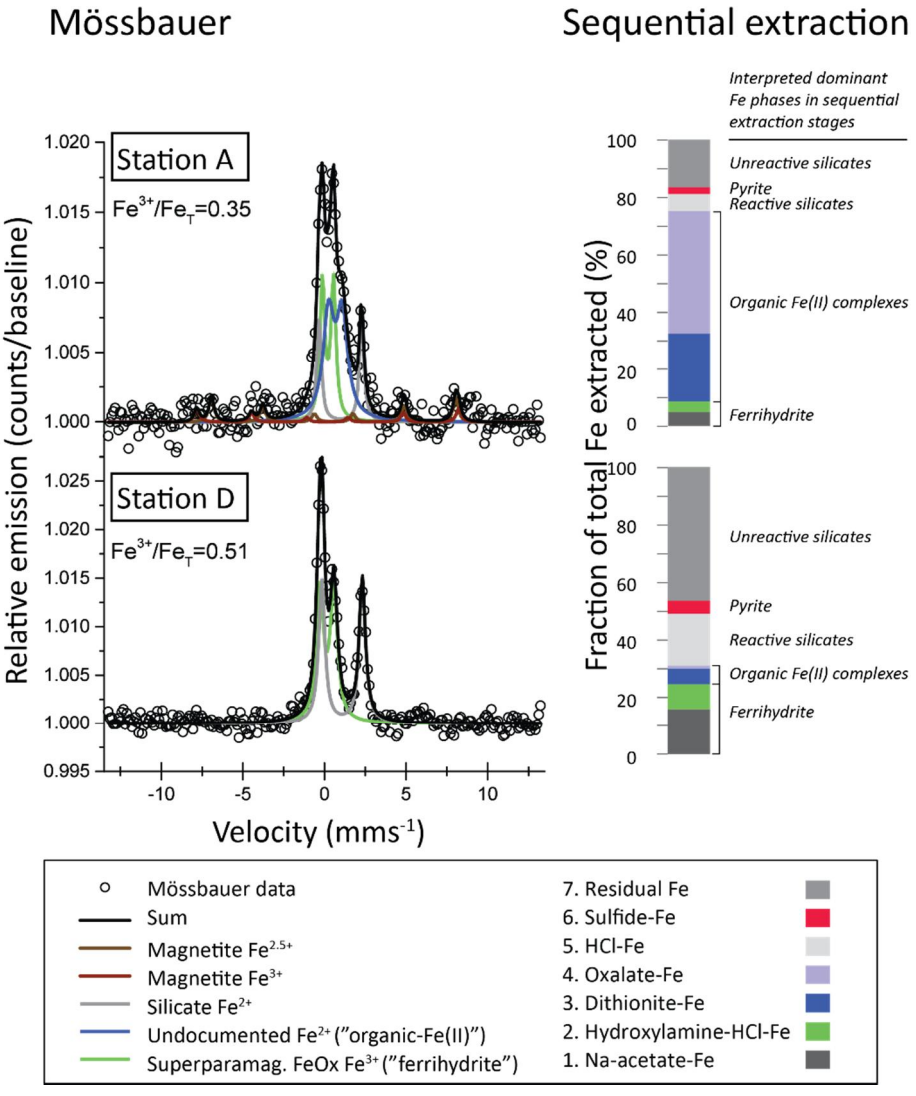

Figure 5. (left) Mössbauer spectra of powdered surface sediments (0–1 cm) from Stations A and D, sampled in 2015 (0.0 and 7.5 km respectively from the river mouth of the Mustionjoki transect). Sub-spectra of Fe-bearing sedimentary components (colored lines) were combined using a linear combination fitting (LCF) routine to generate a sum spectrum (black line) with the closest fit to the raw data (circles). Concentrations of each component, and Fe^{2+}/Fe_T ratios, were estimated from the LCF model. Mössbauer fitting parameters are listed in Table 3. (right) Sequential extraction results from the same samples, showing the complete speciation of Fe according to the method of Poulton and Canfield (2005) and an additional extraction for sulfide-bound Fe. The interpreted dominant Fe phases in each stage of the sequential extraction are given in the right column.

Biogeosciences Discuss., doi:10.5194/bg-2017-181, 2017
Manuscript under review for journal Biogeosciences
Discussion started: 19 May 2017

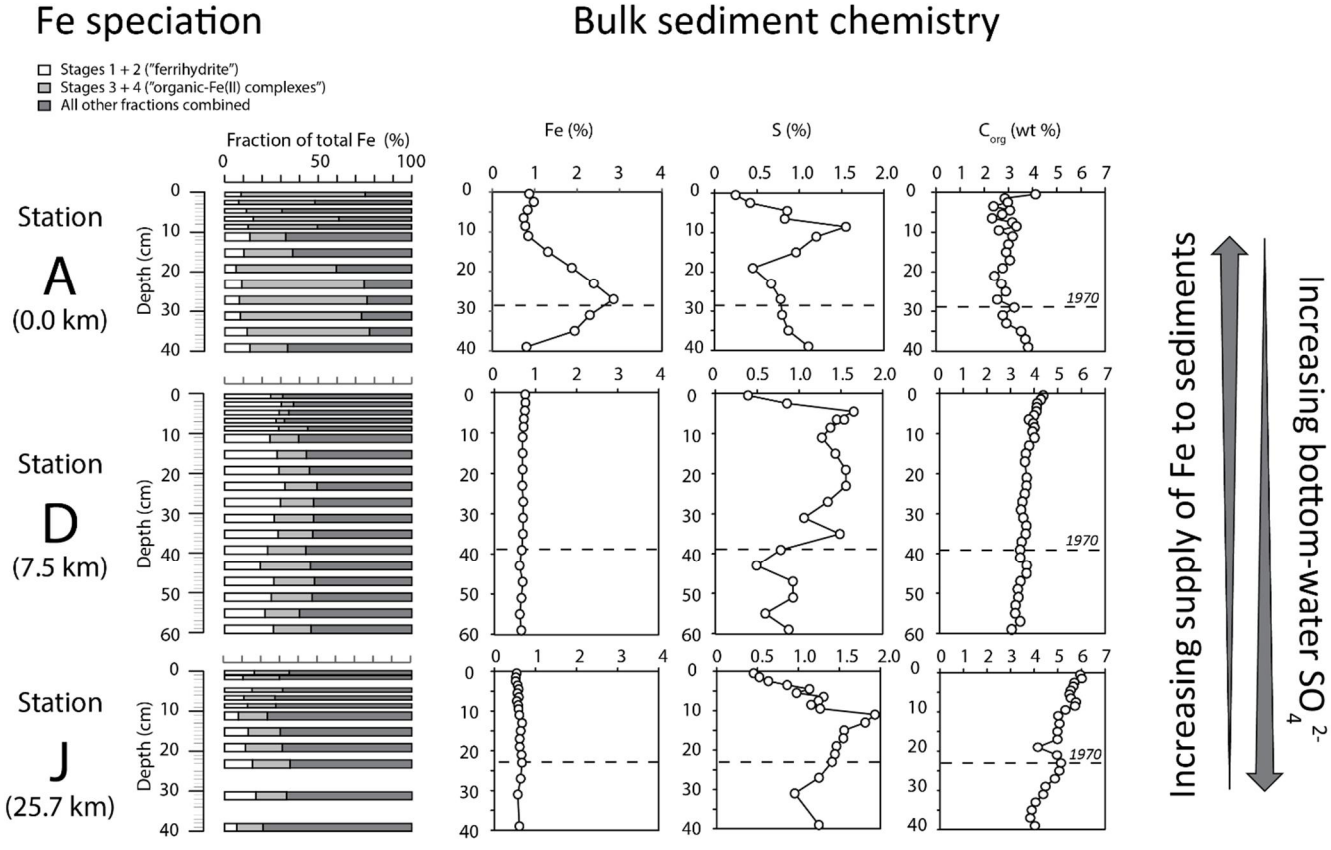

Figure 6. (left) Down-core operational Fe speciation for Stations A, D, and J (0.0, 7.5 and 25.7 km respectively from the river mouth of the Mustionjoki transect), derived from sequential extraction by the method of Poulton and Canfield (2005) and an additional extraction for sulfide-bound Fe. Thickness of bars corresponds to thickness of sampled interval (i.e. 1 or 2 cm). Note that not all depth intervals were sampled. (right) Down-core bulk chemical profiles from the same cores. Total Fe and S were determined by ICP-OES analysis of powdered sediments digested by $HF+HClO_4+HNO_3$, while C_{org} was determined by thermal combustion of powdered sediments (see text for further details). The depth interval corresponding to 1970 is estimated from the peak in concentrations of total lead (Pb_{tot}) as determined by ICP-OES (see Supplementary information).

Biogeosciences Discuss., doi:10.5194/bg-2017-181, 2017
Manuscript under review for journal Biogeosciences
Discussion started: 19 May 2017

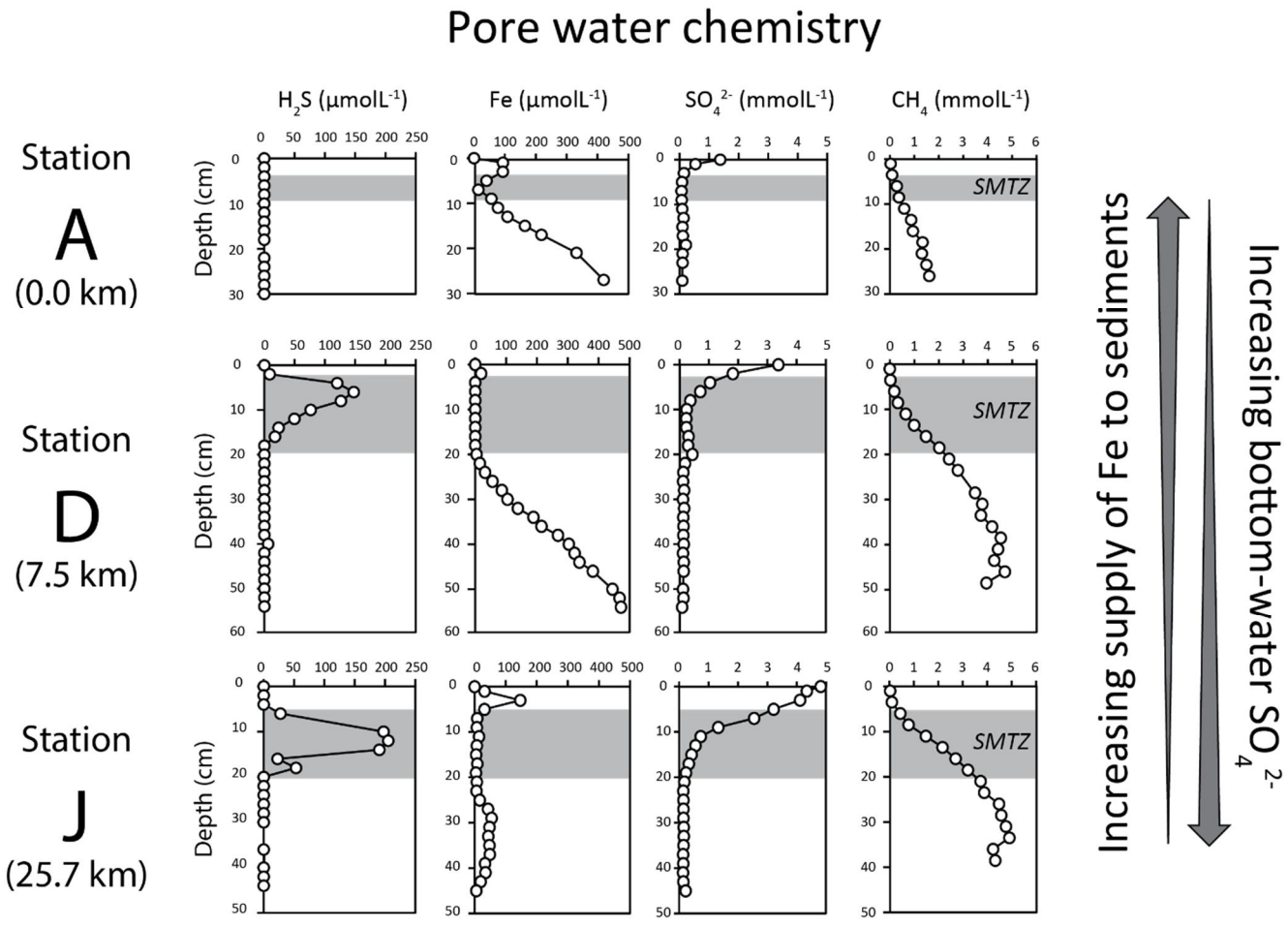

Figure 7. Pore water chemical profiles from Stations A, D and J (0.0, 7.5 and 25.7 km respectively from the river mouth of the Mustionjoki transect). See text for methodological details. SMTZ = Sulfate-Methane Transition Zone.

Biogeosciences Discuss., doi:10.5194/bg-2017-181, 2017
Manuscript under review for journal Biogeosciences
Discussion started: 19 May 2017

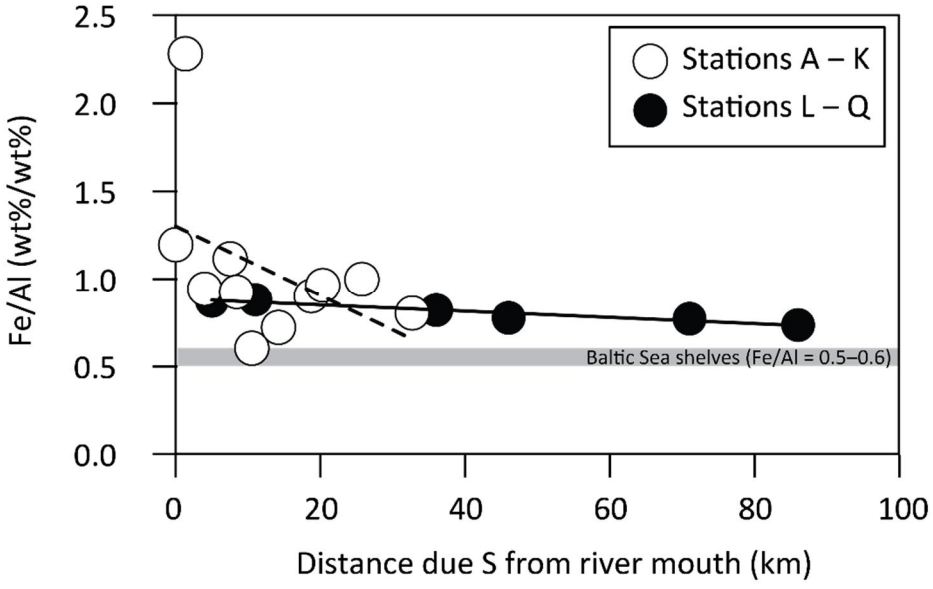

Figure 8. Fe/Al weight ratios for surface sediment samples along the Mustionjoki (0–2 cm; Stations A–K) and Paimionjoki (0–1 cm; Stations L–Q) transects. Linear regression lines are shown for each transect. Typical values for surface sediments of the Baltic Sea shelves (Fe/Al =0.5-0.6, Eastern Gotland basin, Lenz et al., 2015) are shown for comparison.